ENGINEERING OF
BIOMATERIALS
INŻYNIERIA BIOMATERIAŁÓW

ENGINEERING OF BIOMATERIALS

ENGINEERING OF BIO●MATERIALS

Wskazówki dla autorów

1. Prace do opublikowania w kwartalniku „Engineering of Biomaterials / Inżynieria Biomateriałów" przyjmowane będą wyłącznie w języku angielskim.

2. Wszystkie nadsyłane artykuły są recenzowane.

3. Materiały do druku prosimy przysyłać za pomocą systemu online (www.biomaterials.pl).

4. Struktura artykułu:
• TYTUŁ • Autorzy i instytucje • Streszczenie (200-250 słów) • Słowa kluczowe (4-6) • Wprowadzenie • Materiały i metody • Wyniki i dyskusja • Wnioski • Podziękowania • Piśmiennictwo

5. Autorzy przesyłają pełną wersję artykułu, łącznie z ilustracjami, tabelami, podpisami i literaturą w jednym pliku. Artykuł w tej formie przesyłany jest do recenzentów. Dodatkowo autorzy proszeni są o przesłanie materiałów ilustracyjnych (rysunki, schematy, fotografie, wykresy) w oddzielnych plikach (format np. .jpg, .gif., .tiff, .bmp). Rozdzielczość rysunków min. 300 dpi. Wszystkie rysunki i wykresy powinny być czarno-białe lub w odcieniach szarości i ponumerowane cyframi arabskimi. W tekście należy umieścić odnośniki do rysunków i tabel.

6. Na końcu artykułu należy podać wykaz piśmiennictwa w kolejności cytowania w tekście i kolejno ponumerowany.

7. Redakcja zastrzega sobie prawo wprowadzenia do opracowań autorskich zmian terminologicznych, poprawek redakcyjnych, stylistycznych, w celu dostosowania artykułu do norm przyjętych w naszym czasopiśmie. Zmiany i uzupełnienia merytoryczne będą dokonywane w uzgodnieniu z autorem.

8. Opinia lub uwagi recenzentów będą przekazywane Autorowi do ustosunkowania się. Nie dostarczenie poprawionego artykułu w terminie oznacza rezygnację Autora z publikacji pracy w naszym czasopiśmie.

9. Za publikację artykułów redakcja nie płaci honorarium autorskiego.

10. Adres redakcji:
Czasopismo
„Engineering of Biomaterials / Inżynieria Biomateriałów"
Akademia Górniczo-Hutnicza im. St. Staszica
Wydział Inżynierii Materiałowej i Ceramiki
al. Mickiewicza 30/A-3, 30-059 Kraków
tel. (48) 12 617 44 48, 12 617 25 61
e-mail: epamula@agh.edu.pl, kabe@agh.edu.pl

Szczegółowe informacje dotyczące przygotowania manuskryptu oraz procedury recenzowania dostępne są na stronie internetowej czasopisma:
www.biomaterials.pl

Instructions for authors

1. Papers for publication in quarterly journal „Engineering of Biomaterials / Inżynieria Biomateriałów" should be written in English.

2. All articles are reviewed.

3. Manuscripts should be submitted to editorial office through online submission system (www.biomaterials.pl).

4. A manuscript should be organized in the following order:
• TITLE • Authors and affiliations • Abstract (200-250 words) • Keywords (4-6) • Introduction • Materials and Methods • Results and Discussion • Conclusions • Acknowledgements • References

5. All illustrations, figures, tables, graphs etc. preferably in black and white or grey scale should be additionally sent as separate electronic files (format .jpg, .gif, .tiff, .bmp). High-resolution figures are required for publication, at least 300 dpi. All figures must be numbered in the order in which they appear in the paper and captioned below. They should be referenced in the text. The captions of all figures should be submitted on a separate sheet.

6. References should be listed at the end of the article. Number the references consecutively in the order in which they are first mentioned in the text.

7. The Editors reserve the right to improve manuscripts on grammar and style and to modify the manuscripts to fit in with the style of the journal. If extensive alterations are required, the manuscript will be returned to the authors for revision.

8. Opinion or notes of reviewers will be transferred to the author. If the corrected article will not be supplied on time, it means that the author has resigned from publication of work in our journal.

9. Editorial does not pay author honorarium for publication of article.

10. Address of editorial office:
Journal
„Engineering of Biomaterials / Inżynieria Biomateriałów"
AGH University of Science and Technology
Faculty of Materials Science and Ceramics
30/A-3, Mickiewicz Av., 30-059 Krakow, Poland
tel. (48) 12) 617 44 48, 12 617 25 61
e-mail: epamula@agh.edu.pl, kabe@agh.edu.pl

Detailed information concerning manuscript preparation and review process are available at the journal's website:
www.biomaterials.pl

STUDIA PODYPLOMOWE
Biomateriały – Materiały dla Medycyny
2022/2023

Organizator: Akademia Górniczo-Hutnicza im. Stanisława Staszica w Krakowie Wydział Inżynierii Materiałowej i Ceramiki Katedra Biomateriałów i Kompozytów **Kierownik:** prof. dr hab. inż. Elżbieta Pamuła **Sekretarz:** dr inż. Małgorzata Krok-Borkowicz	**Adres:** 30-059 Kraków, Al. Mickiewicza 30 Pawilon A3, p. 208 lub p. 210 tel. 12 617 44 48, 12 617 23 38 email: epamula@agh.edu.pl; krok@agh.edu.pl https://www.agh.edu.pl/ksztalcenie/oferta-ksztalcenia/ studia-podyplomowe-kursy-doksztalcajace-i-szkolenia/ biomaterialy-materialy-dla-medycyny/

Charakterystyka:

Tematyka prezentowana w trakcie zajęć obejmuje przegląd wszystkich grup materiałów dla zastosowań medycznych: metalicznych, ceramicznych, polimerowych, węglowych i kompozytowych. Słuchacze zapoznają się z metodami projektowania i wytwarzania biomateriałów a następnie możliwościami analizy ich właściwości mechanicznych, właściwości fizykochemicznych (laboratoria z metod badań: elektronowa mikroskopia skaningowa, mikroskopia sił atomowych, spektroskopia w podczerwieni, badania energii powierzchniowej i zwilżalności) i właściwości biologicznych (badania: *in vitro* i *in vivo*). Omawiane są regulacje prawne i aspekty etyczne związane z badaniami na zwierzętach i badaniami klinicznymi (norma EU ISO 10993). Słuchacze zapoznają się z najnowszymi osiągnięciami w zakresie nowoczesnych nośników leków, medycyny regeneracyjnej i inżynierii tkankowej.

Sylwetka absolwenta:

Studia adresowane są do absolwentów uczelni technicznych (inżynieria materiałowa, technologia chemiczna), przyrodniczych (chemia, biologia, biotechnologia) a także medycznych, stomatologicznych, farmaceutycznych i weterynaryjnych, pragnących zdobyć, poszerzyć i ugruntować wiedzę z zakresu inżynierii biomateriałów i nowoczesnych materiałów dla medycyny. Słuchacze zdobywają i/lub pogłębiają wiedzę z zakresu inżynierii biomateriałów. Po zakończeniu studiów wykazują się znajomością budowy, właściwości i sposobu otrzymywania materiałów przeznaczonych dla medycyny. Potrafią analizować wyniki badań i przekładać je na zachowanie się biomateriału w warunkach żywego organizmu. Ponadto słuchacze wprowadzani są w zagadnienia dotyczące wymagań normowych, etycznych i prawnych niezbędnych do wprowadzenia nowego materiału na rynek. Ukończenie studiów pozwala na nabycie umiejętności przygotowywania wniosków do Komisji Etycznych i doboru metod badawczych w zakresie analizy biozgodności materiałów.

Zasady naboru:

Termin zgłoszeń: od 20.09.2022 do 20.10.2022 (liczba miejsc ograniczona - decyduje kolejność zgłoszeń)
Wymagane dokumenty: dyplom ukończenia szkoły wyższej
Osoby przyjmujące zgłoszenia:
prof. dr hab. inż. Elżbieta Pamuła (pawilon A3, p. 208, tel. 12 617 44 48, e-mail: epamula@agh.edu.pl)
dr inż. Małgorzata Krok-Borkowicz (pawilon A3, p. 210, tel. 12 617 23 38, e-mail: krok@agh.edu.pl)

Czas trwania: 2 semestry (od XI 2022 r. do VI 2023 r.) 8 zjazdów (soboty-niedziele) 1 raz w miesiącu przewidywana liczba godzin: 160	**Opłaty:** 3 000 zł (za dwa semestry)

31st Biomaterials in Medicine and Veterinary Medicine

Annual Conference

13 – 16 October 2022 Rytro, Poland

POLISH SOCIETY FOR BIOMATERIALS

SAVE THE DATE

13-16

OCTOBER

2022

www.biomat.agh.edu.pl

REGISTER
AND
SUBMIT
AN ABSTRACT

ENGINEERING OF BIOMATERIALS

SPIS TREŚCI
CONTENTS

ENGINEERING OF BIOMATERIALS

CHEMICAL STABILITY ASSESSMENT OF SOFT MAGNETIC COMPOSITES FOR BIOMEDICAL APPLICATIONS

Anna Powojska[1]* , Joanna Niewęgłowska[1] ,
Sylwia Suska[1] , Adelio Cavadas[2,3] ,
Joanna Mystkowska[1]

[1] Institute of Biomedical Engineering,
Faculty of Mechanical Engineering,
Bialystok University of Technology,
ul. Wiejska 45C, 15-351 Bialystok, Poland
[2] ProMetheus, Institute Polytechnic of Viana
do Castelo, 4900-347 Viana do Castelo, Portugal
[3] Transport Phenomena Research Center,
Faculty of Engineering, University of Porto,
Rua Dr. Roberto Frias s/N, 4200-465 Porto, Portugal
*e-mail: a.powojska@doktoranci.pb.edu.pl

Abstract

Silicone-based elastic composites with a metallic filler have been strongly developed in recent years. These materials are considered applicable in many fields of science, including medicine. The advantageous mechanical parameters provided by the NdFeB micropowder reinforcement are balanced by the elasticity and biocompatibility guaranteed by the silicone matrix. So far, there have been several reports regarding such composites' properties important from the biomedical point of view. The article deals with the physicochemical parameters of the new material for medical applications as well as the properties of the incubation liquid. The aim of the work was to determine effects of both the magnetic particles content (0, 30, 50, 70 wt%) and the incubation process under physiological conditions on the physicochemical properties of the material and the solution after incubation. The samples were incubated for various periods of time (8, 16 and 24 weeks) at the temperature of 37°C in a 0.9 wt% NaCl solution. The density, water contact angle, and water absorption of the materials were measured. The electrolytic conductivity, pH value, redox potential, surface tension, and kinematic viscosity were determined for the liquids after the materials incubation. The results obtained for pure silicone and the silicone-based composite reinforced with NdFeB microparticles were compared. The results indicate that incubation affects the samples and liquids, changing their physiochemical properties. For composites, the density decreased, which results in a noticeable concentration of the examined elements in the solutions.

Keywords: *silicone-based composite, magnetic material, physicochemical properties, incubation, ICP-MS analysis*

Introduction

One of the significant directions of progress in biomedical engineering is the need to develop new biomaterials. However, many aspects must be considered to provide safe and useful materials [1]. Despite the chemical composition, the fabrication method is essential in assessing biomaterial's properties [2,3]. In the last few years, there has been an increasing interest in elastic materials endowed with some additional features. Thus, silicones are widely used for applications in medicine. Polydimethylsiloxane (PDMS) is a well-known type of silicone that belongs to the group of siloxanes [4]. It is altered to manufacture stretchable structures, elements of surgical instruments, microfluidic devices, or drug delivery systems [5,6]. PDMS is also used for tissue simulating optical phantoms useful in the development of biomedical engineering technologies [3] and for medical electronics, e.g., electrochemical sensors [7]. Its structural biocompatibility, biostability, and various applications in medicine, were the main reasons for choosing PDMS as a matrix to prepare magnetic powder-based composites in this work [6].

Soft composites can be reinforced with various fillers. One of the groups of filling materials that is becoming increasingly important in materials science is metal alloys with magnetic properties. The balance between the structure flexibility and the ability to move in a magnetic field can be obtained in these composites [8]. Magnetic particles with different shapes and chemical composition are used in biomedical engineering [9-11]. The most popular element showing ferromagnetic behaviour is iron (Fe). Iron is part of many compounds for medical purpose, such as magnetite (Fe_3O_4) or maghemite (γFe_2O_3) [12]. This element is the main component of neodymium magnet (NdFeB). Applications of NdFeB magnets in medical sciences increased in the last decades [11,13,14]. Silicone-based composites reinforced with magnetic particles, especially with NdFeB, are of great interest to researchers from all over the world. Those materials combine elasticity and biocompatibility supported by an organic matrix, and the possibility of the material remote control provided by a filler with magnetic properties. Soft magnetic composites can act as microrobots for precise surgeries. They can also play a role in targeted drug delivery, where precision is crucial [8,15,16]. Many cancer therapies are specific and can be delivered via remotely controlled structures. In this case, drugs are applied to the composite surface. The drug activation may be induced by a magnetic field of a certain value [17,18].

The assessment of new magnetic materials in medicine, apart from their mechanical, thermal and functional properties, also includes their biocompatibility study and impact on the human body. One of the parameters is the influence of physiological fluids on the physicochemical properties of composites. The tendency to release the elements of the magnetic filler from the composite to the environment has to be considered as well. The most commonly used solution for the biomaterials incubation is a sodium chloride solution (0.9 wt% NaCl) [19]. Studies are performed mostly to analyze the material behaviour under specific conditions. The material properties change with the incubation time in the simulated physiological environment is also evaluated [20]. The biomaterial should retain its properties and therefore should not release toxic compounds into the body [21,22].

NdFeB magnets have already been well-examined for medical applications and are considered to be cytotoxic to certain types of animal or human cells. The tests performed *in vitro* for mucosal fibroblasts showed high cytotoxicity in contact with neodymium [23,24]. Neodymium particles, when not handled with care, can come closer to each other inside the body, causing harmful injuries. It is proven that the presence of neodymium in the human body can damage the liver or cause lung embolism [25,26]. Although, there are no reports regarding the maximum allowable concentration of neodymium, it has to be considered if the component is not rejected by the human or animal body. Iron is an essential element for the proper functioning of the body. It is found in human haemoglobin, cells, and enzymes. Iron deficiency can be dangerous for human health [27]. Boron is a trace element in the human body, delivered with water and food. It can be toxic when the boron intake exceeds 0.75 mg/day for infants, 1.34 mg/day for 50 year-old men, and 1.39 mg/day for nursing mothers [28,29]. Biodegradation and biocorrosion studies for NdFeB magnets defined the neutral or mild behaviour of the material in the microbial environment [13,30].

The main goal of the presented study was to determine physicochemical properties of both the PDMS-based material and the solution after the incubation process. Another goal was to analyze the influence of different powder content on the materials properties. Finally, the research should reveal whether the incubation time affects the chosen characteristics of both the material and the solution.

Materials and Methods

The examined materials were PDMS-based composites with NdFeB micropowder as a filler. A silicone with the trade name Sylgard 184 (Dow Corning, Midland, MI, USA) was used as an organic matrix. This polymer was supplied in a two-component form: an elastomer and a curing agent. The ingredients were mixed in a weight ratio of 10:1. A metallic micropowder with magnetic properties with the trade name MQFP-14-12 (Magnequench, Singapore, Singapore) was used as a reinforcement. The size distribution given by a production company is of d50 = 25 μm. The chemical composition of the metal alloy is presented in TABLE 1.

The composite manufacturing process started with the silicone matrix preparation. About 20 g of elastomeric liquid was mixed with approximately 2 g of the liquid curing agent to obtain a proper silicone. Then, the material was immediately transferred into four separate Petri dishes. The reinforcement was added to the second, third and fourth dish, in order to obtain composites with 30, 50, and 70 wt% of a filler, respectively. The components for each composite were hand-mixed to obtain a homogenous mixture. In the next step, each material was poured on a PTFE mat and put into a vacuum dryer. Gases entrapped inside the composite were released. The degassed composites were cured in a LabEcon 300 hydraulic press (Fontijne, Vlaardingen, The Netherlands) for 20 min at the fixed temperature (100°C). The cured materials were cut into uniform 9 mm diameter discs of a 1 mm thickness. The prepared samples were weighed before immersing them in a solution.

The solution for the simulation under *in vitro* conditions was 0.9 wt% sodium chloride (NaCl, Sigma Aldrich, St. Louis, MO, USA) in ultrapure Milli-Q water (Merck Milipore, Darmstadt, Germany). The water was mixed with NaCl and then the physicochemical properties of the conditioning liquid were determined to obtain the reference sample characteristics. The composite samples were placed in plastic containers. Each composite and pure PDMS were conditioned separately.

TABLE 1. Chemical composition of the micropowder.

Element	Symbol	Percentage
Neodymium	Nd	26%
Boron	B	1%
Niobum	Nb	1.9%
Iron	Fe	71.1%

TABLE 2. Designation of samples.

Designation	Incubation time [weeks]	Concentration of filler [wt%]
0-0	0	0
0-8	8	0
0-16	16	0
0-24	24	0
30-0	0	30
30-8	8	30
30-16	16	30
30-24	24	30
50-0	0	50
50-8	8	50
50-16	16	50
50-24	24	50
70-0	0	70
70-8	8	70
70-16	16	70
70-24	24	70

Three sets of each type of examined material were prepared for investigating the effects of different incubation times. The samples were immersed in the sodium chloride solution with a weight/volume ratio of 1:10. The samples designations are presented in TABLE 2. It should be noticed that the control samples of solution were incubated in separate plastic containers for the same time periods as the materials for incubation.

The samples were conditioned in a laboratory incubator at a constant temperature of 37 ± 0.5°C for 8, 16 and 24 weeks. After each period of time, the designated samples were taken out and dried. The control samples i.e. pure silicone and the composite materials were not subjected to the incubation process at all. Having been incubated, the samples were dried in air at the temperature of 22 ± 1°C and the humidity of 50%. After the materials were removed, the incubation solutions were examined regarding their pH, conductivity, redox potential, surface tension, and kinematic viscosity. The physicochemical properties of materials (density, wettability, water absorption) were evaluated as well.

The SevenMulti (Mettler Toledo, Columbus, OH, USA) multifunctional ionoconductometr with dedicated electrodes was used to measure the pH, conductivity, and redox potential. The surface tension tests were performed using a balance (Mettler Toledo, Columbus, OH, USA) with a platinum ring and the STA1 tensiometer (Sinterface, Berlin, Germany) [31]. The surface tension value (γ) was calculated from the formula (1):

$$\gamma = \frac{F}{4\pi R} \tag{1}$$

where F is the force needed to separate the ring from the solution surface [N], and R is the radius of the measuring ring [m].

The kinematic viscosity of solutions was determined using the iVisc system (LAUDA Scientific, Lauda-Königshofen, Germany) shown in FIG. 1. The system consists of the Ubbelohde glass capillary and a self-priming handle with an optical system for the liquid flow measurement. The capillary was immersed in a thermostat, so the solution temperature was in the same range for all the experiments. The measurements were performed using software connected to a device. The evaluation of kinematic viscosity is person-independent, which makes those calculations very precise. The physicochemical tests were performed at the temperature $25 \pm 1°C$ and the measurements were repeated five times for each solution.
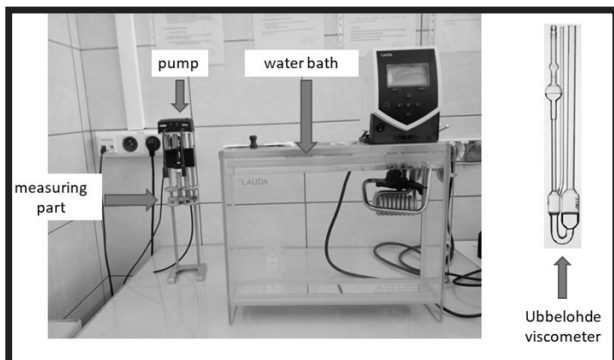
FIG. 1. iVisc system for kinematic viscosity determination.

The elements concentration in the solutions was determined using inductively coupled plasma-mass spectrometry (ICP-MS). This type of spectrometry is used to measure trace elements in biological solutions by comparing their concentration with standards. The ICP-MS analysis of the solutions after conditioning was performed using the Triple Quadrupole ICP-MS (8800 ICP-QQQ, Agilent Technologies, Singapore) fitted with MicroMist nebulizer, Scott-type double pass spray chamber Peltier cooled, nickel sampler and skimmer cones, and collision/reaction cell (octopole reaction system ORS3) [32]. The ICP-MS method was used to determine iron, neodymium, boron, and niobium with interfering elements in the model solutions and the experimental samples.

The samples density (d) was measured by the hydrostatic method. The experiment was conducted using the balance (Mettler Toledo, Columbus, OH, USA) with the special equipment. The procedure is that the weight of the sample is recorded first on a plate in air, then in water. The density was automatically calculated by the balance software. Density tests were performed five times for each sample. The wettability of the materials surface was determined using the Contact Angle Goniometer (Ossila, Sheffield, UK). Wettability is defined by the contact angle (Θ) between the surface of the examined material and a droplet of ultrapure water on the surface. The acquired images of bare PDMS and PDMS-based composites were analyzed with the Ossila Contact Angle software using a tangent method [33]. For each sample, the contact angle was measured five times. The water absorption (W) was determined using a balance with a high sensitivity of 0.01 mg (Mettler Toledo, Columbus, OH, USA). The measurements compared the samples weight before and after incubation. Each sample was weighted before immersion in a medium and after a set incubation time. The experiment was followed by a day of drying at room temperature of $22 \pm 1°C$ and 50% humidity. The water absorption value is a percentage gain weight of the examined sample.

The obtained results are presented in the form of mean values ± standard deviations. To determine the significance level for the conducted studies, the one-way ANOVA and Tukey's post-hoc analysis were performed. The statistical analysis was performed with Statistica 13.1 software. The value of $p < 0.05$, and the significance level of $\alpha = 0.05$ were assumed. Probability values less than 0.05 were considered statistically significant.

Results and Discussion

The properties of sodium chloride solutions after the incubation of PDMS-based composites with magnetic powder were determined. In FIG. 2 the results for the pH value (FIG. 2A), electrolytic conductivity (FIG. 2B), redox potential (FIG. 2C) and surface tension (FIG. 2D) measurements of solutions *vs* time in weeks are presented. These properties are crucial for the material's potential application in biomedical engineering, especially when considering the contact of material with blood and other body fluids. The tests are aimed at verifying the influence of the material on the environment they are supposed to work in. Characterization of the solutions after incubation is essential to identify any biological hazards and show the compliance with regulatory expectations. It is a key issue in terms of accelerating the material or device development in certain conditions.

The initial pH of the sodium chloride was about 7.05 ± 0.02 and it was virtually invariable over the incubation time. An increase in pH of about 0.15 was observed for the solutions after incubation of pure PDMS. With the higher percentage of magnetic filler, the differences were more visible. For the solutions the composites were immersed in, the pH value increased significantly as the incubation time was prolonged. After 24 weeks of incubation, the solution for the 30-24 sample was characterized by the pH increase of about 0.20, the 50-24 sample solution was characterized by the increase of about 0.30 and for the 70-24 solution the pH increase of about 0.50 was observed. The obtained results followed the rule: the higher percentage of magnetic filler, the higher increase in pH value (FIG. 2A), which indicates the interaction between the solution and the incubated composites. The pH value increase can be caused by the chemical processes occurring on the composite surface during the incubation. The oxides, which are formed on the basis of elements separated from the material, might change the pH of the solution. It has to be noticed that the observed pH value was slightly higher than the pH of natural saliva (7.2) [34].

The electrolytic conductivity (k) value of the freshly prepared 0.9 wt% NaCl solution was 13.54 mS/cm. Electrolytic conductivity also showed that the longer incubation time, the higher value of this parameter was obtained. The lowest difference was observed for the control sample with the change of 0.3 mS/cm. The higher changes were noticed for the 70-0 and 70-24 samples solutions differing about 5.1 mS/cm. The interaction between the composite with the 70 wt% of the filler was presumably intensive, hence such changes could have been observed. The lower filler concentration in a composite, the lower changes of the electrolytic conductivity were observed. The change was expected, as the elements in the ionic form could get into solution from the composite.

The redox potential values (E_h) decreased for the solutions after the material incubation, which indicated the intensification of the reduction reactions. For the solutions, where the composites with higher NdFeB content were incubated, the E_h decrease was more significant.
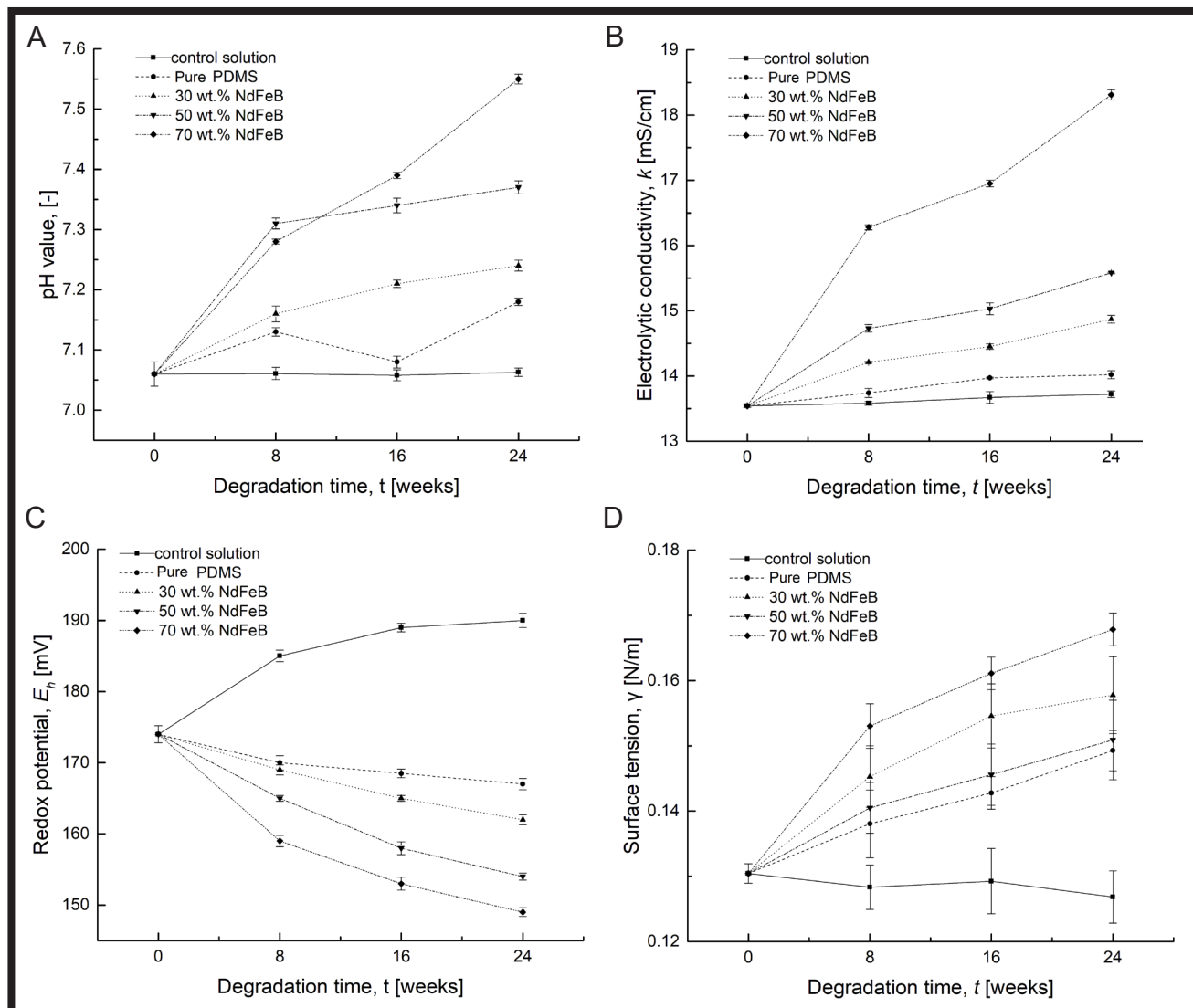
FIG. 2. Results of physiochemical properties of solutions *vs* incubation time: (A) pH value; (B) Electrolytic conductivity; (C) Redox potential; (D) Surface tension.

This change is connected with a higher concentration of elements in solutions that may undergo oxidation or reduction. For the 70-24 solution, E_h was about 25 mV lower, for the 50-24 solution it was 20 mV lower and for the 30-24 solution 10 mV lower in comparison to the freshly prepared solution. The inverse relationship i.e. the E_h value increase was observed for the control sample, where mainly oxidation reactions occurred. For the control solution incubated for 24 weeks (T = 37°C) the E_h value increased by approximately 15 mV. The lower E_h indicates the tendency to perform oxidation reactions, caused by the electron loss in the solution.

The results of the surface tension for the solutions after incubation are presented in FIG. 2D. The tested parameter increased with the materials incubation time and with the higher percentage content of the powder filler. Between the initial value and the value for the 70-24 solution the difference was about 0.035 N/m. Lower differences were observed for solutions where the composites of 50 and 30 wt% addition were incubated. The surface tension of the control NaCl solution decreased with the incubation time for about 0.005 N/m. The change in the surface tension value is affected by the changes in the intermolecular forces system in the examined solution. That might be caused by the release of elements from the composite to the solution. The surface tension increase means that the wettability decreases and causes less adhesion.

The primary value of the kinematic viscosity for the control solution was of 0.00959 cm^2/s and it increased over time. The value grew significantly for the solutions after incubating the 70 wt% NdFeB composite over time (for approximately 0.0025 cm^2/s). The difference for the solutions after incubating the composites of 30 wt% and 50 wt% was of 0.0014 cm^2/s and 0.0018 cm^2/s, respectively. The kinematic viscosity changed with the incubation time, presumably due to the change in the chemical composition of the solutions and the ions diffusion into the solution. The kinematic viscosity was in a linear correlation to the pH value. The data presented in FIG. 3. show the correlation between the kinematic viscosity of solutions (v) and pH value. The data prove the relationship: the higher pH value, the higher kinematic viscosity. Due to the Pearson's r (0.88) and adjusted R-square (0.76) coefficients, the data fit the linear regression model. The data for pH value *vs* kinematic viscosity are correlated. At the higher pH values, the solutions viscosity is expected to increase due to the new compounds in the incubation liquid and the presence of ions.
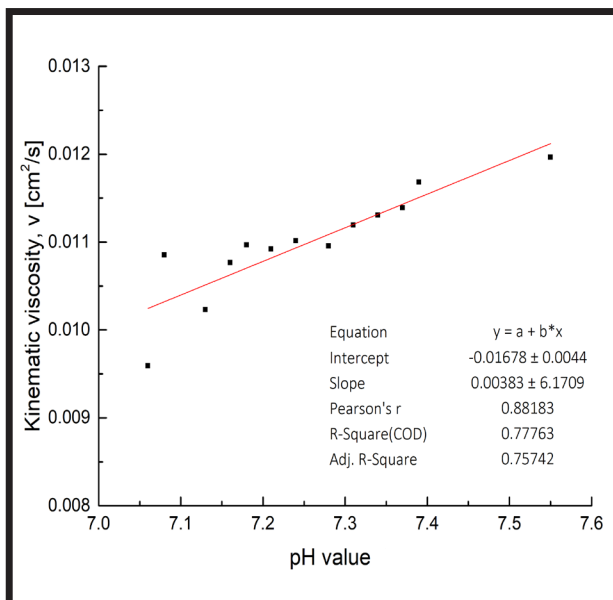
FIG. 3. The correlation between the kinematic viscosity (v) and pH value of examined solutions.

The chemical composition and concentration of selected elements in the solutions after the material incubation were investigated. The results of the ICP-MS analysis are presented in TABLE 3. The presence of Nd, Fe, B, and Nb in the solution after incubation was caused by the release of elements. The concentrations of each element varied and the following changes were observed. For boron, the lowest concentration was observed for the solution after 24 weeks incubation of the composite with 70 wt% NdFeB reinforcement. The highest value was noticed for the solution after conditioning the composite for 16 weeks. Surprisingly, the concentration of Fe in the solutions after incubation of the 70 wt% composites, despite repeated experiments, was under the detection limit for this element and the method combined.

The content of elements in the solutions after incubation of all the tested composites (30, 50 and 70 wt% of magnetic powder) and the total content of all the elements for each tested composite are presented in FIG. 4. The highest diffusion of elements into the solutions was noted for the samples indexed as 30-24, 50-8, and 50-16. The boron concentration was relatively high (5 µg/ml or more) for all the solutions (18 µg/ml or more). The iron concentration was high for the solutions indexed by 30-24, 50-8, and 50-16. The neodymium content was the highest for the 70-16 solution. The time of exposure did not affect the chemical composition of the solution.

TABLE. 3. Results for ICP-MS analysis (LOD is the limit of detection).

| Solution Sample	B Concentration [µg/ml]	Fe Concentration [µg/ml]	Nd Concentration [µg/ml]	Nb Concentration [ng/ml]
0-0	0.00	<LOD	0.018	<LOD
0-8	0.00	<LOD	0.035	<LOD
0-16	0.07	<LOD	0.035	<LOD
0-24	0.00	<LOD	0.087	<LOD
30-8	14.26	7.16	1.614	3.83
30-16	12.13	4.05	0.673	1.37
30-24	15.00	18.01	1.203	1.01
50-8	10.69	18.73	0.928	0.33
50-16	10.75	20.04	0.860	4.54
50-24	14.95	2.70	0.698	0.27
70-8	17.40	<LOD	0.251	0.30
70-16	20.59	<LOD	8.112	9.61
70-24	4.63	<LOD	0.249	1.49
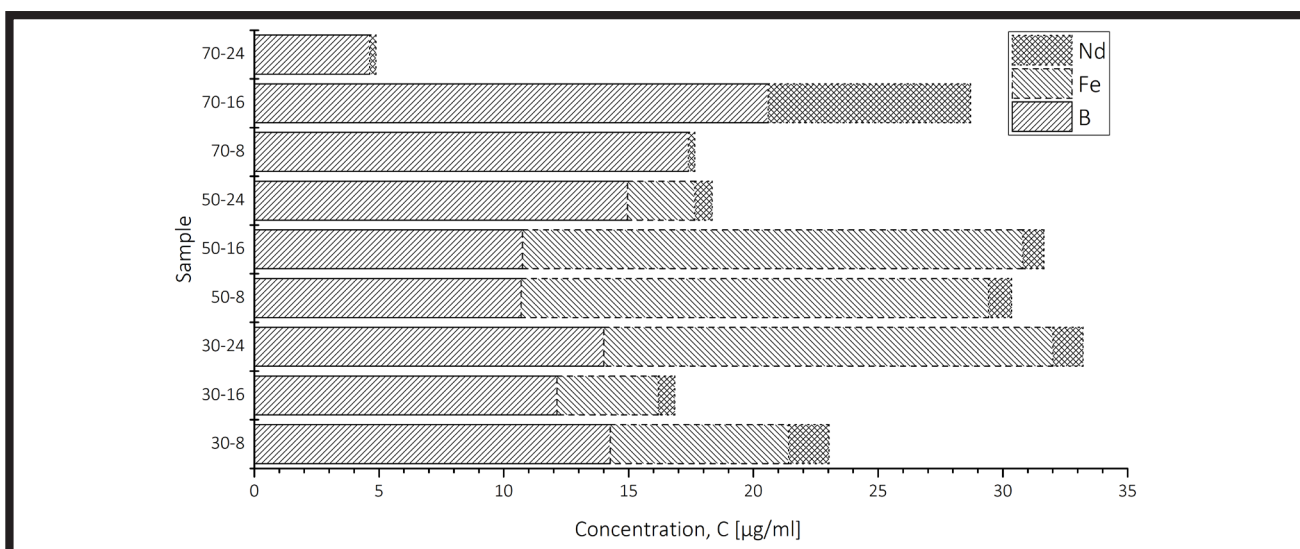
FIG. 4. Concentration of Nd, Fe and B in solutions for different materials and incubation times.
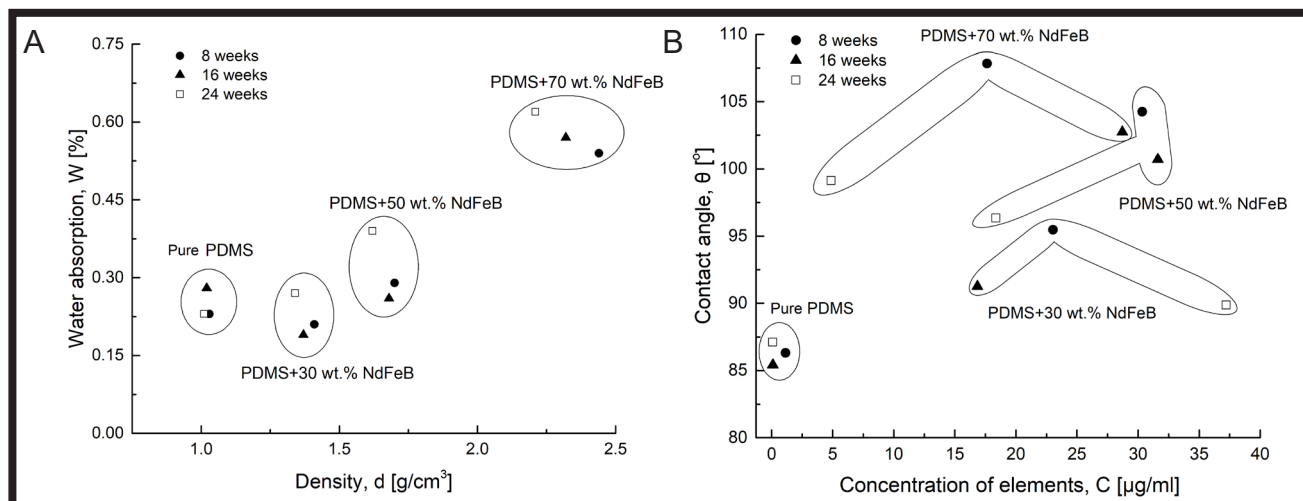
FIG. 5. The correlation between chosen parameters. (A) The water absorption (W) vs density (d) for the examined materials. (B) The contact angle of surface of materials (θ) vs the concentration of elements in solution (C).

The results of water absorption by the materials as a function of density are presented in FIG. 5A. The analysis of the data shows that the composites density is highly dependent on the percentage of composite filler. The presented results indicate that with the incubation time, the density decreased for each composite, which might result from the ions release to the solution and changes in the internal structure of the composite. The water absorption was less than 1% of weight of the sample for the examined composites. It was observed that for more dense materials the water absorption was higher and for the composites the water absorption increased with the incubation time.

It was expected that the contact angle value would change due to the elements diffusion to the contact solution. The relationship between those properties are shown in the graph (FIG. 5B). At first, it can be noticed that the samples wettability depends on the filler concentration in a composite. For the higher percentage of the metal filler, the more hydrophobic surface was obtained. Another relationship is connected with the incubation time. Longer incubation resulted in a lower contact angle for all the examined materials. It may be observed that there is no significant difference in a contact angle results between 16 and 24 weeks of incubation. Presumably, the impact of the solution reduces with time. The contact angle for pure PDMS leads to a conclusion that it is less hydrophobic than the PDMS-based composites. The changes between non-incubated composites and the materials after 24-week incubation is of a few degrees, for 30-0 and 30-24 it is around 8.5°, for 50-0 and 50-24 it is around 16.5°, for 70-0 and 70-24 it is around 23.5°. The contact angle obtained for pure PDMS is of a lower range than the data reported in the literature (107-116°). This can be caused by different manufacturing methods and the surface treatment [35-37].

Conclusions

The combination of the PDMS silicone and NdFeB micropowder can provide soft composite with advantageous properties. The presented data obtained for the examined materials show that the addition of metal powder results in the water contact angle and density increase.

The changes in a chemical composition of the conditioning solution are observed. The elements from the incubated samples are released into the solution, causing the increase in pH, redox potential and electrolytic conductivity values.

The ICP-MS analysis showed that the concentration of the elements is of a few µg/ml. That seems to be in a low range, but it is important from biomedical point of view. Potential applications can be considered after the reduction of elements release. The results show that an additional coating is needed. Special features of coating e.g. antibacterial properties or hydrophobic surface can improve composites characteristics.

The influence of the incubation solution on the material properties is noticeable. The density and water contact angle decrease, changing the ability of a material to work in a biological environment. For biomaterials the stability of the properties is crucial and has to be considered in fabrication. An additional coating for the composite surface can prevent from chemical decontamination of the environment the composite works in and from the changes in material properties.

The data presented in this work are preliminary investigations of this kind of biomaterials. Additional research is needed to evaluate the materials characteristics, especially biological properties and living cells behavior when in contact with a composite. At the same time, the research and experiments for surface coatings that meet the requirements should be carried out in order to increase the functionality of the material.

Acknowledgements

ORCID iD

A. Powojska: https://orcid.org/0000-0003-3276-0592
J. Niewęgłowska: https://orcid.org/0000-0002-9035-7147
S. Suska: https://orcid.org/0000-0002-6936-7447
A. Cavadas: https://orcid.org/0000-0003-1792-2223
J. Mystkowska: https://orcid.org/0000-0002-3386-146X

References

[1] Mitragotri S., Lahann J.: Physical Approaches to Biomaterial Design. Nature Materials 8(1) (2009) 15-23.

[2] Zehnder J., Knoop E., Bächer M., Thomaszewski B.: Metasilicone. ACM Transactions on Graphics 36(6) (2017) 1-13.

[3] Ayers F., Grant A., Kuo D., Cuccia D. J., Durkin A.J.: Fabrication and Characterization of Silicone-Based Tissue Phantoms with Tunable Optical Properties in the Visible and near Infrared Domain; Nordstrom, R. J.Ed.; https://doi.org/10.1117/12.764969; p 687007.

[4] Kuncova-Kallio J., Kallio P.J.: PDMS and Its Suitability for Analytical Microfluidic Devices. In 2006 International Conference of the IEEE Engineering in Medicine and Biology Society; https://doi.org/10.1109/IEMBS.2006.260465; IEEE; 2486-2489.

[5] Kim J.H., Lau K.T., Shepherd R., Wu Y., Wallace G., Diamond D.: Performance Characteristics of a Polypyrrole Modified Polydimethylsiloxane (PDMS) Membrane Based Microfluidic Pump. Sensors and Actuators A: Physical 148(1) (2008) 239-244.

[6] Victor A., Ribeiro J., F. Araújo F.: Study of PDMS Characterization and Its Applications in Biomedicine: A Review. Journal of Mechanical Engineering and Biomechanics 4(1) (2019) 1-9.

[7] Casanova-Moreno J., To J., Yang C.W.T., Turner R.F.B., Bizzotto D., Cheung K.C.: Fabricating Devices with Improved Adhesion between PDMS and Gold-Patterned Glass. Sensors and Actuators B: Chemical 246 (2017) 904-909.

[8] Wang X., Mao G., Ge J., Drack M., Cañón Bermúdez G.S., Wirthl D., Illing R., Kosub T., Bischoff L., Wang C., Fassbender J., Kaltenbrunner M., Makarov D.: Untethered and Ultrafast Soft-Bodied Robots. Communications Materials 1(1) (2020) 67.

[9] Seyfoori A., Ebrahimi S.A.S., Omidian S., Naghib S. M.: Multifunctional Magnetic ZnFe$_2$O$_4$-Hydroxyapatite Nanocomposite Particles for Local Anti-Cancer Drug Delivery and Bacterial Infection Inhibition: An in Vitro Study. Journal of the Taiwan Institute of Chemical Engineers 96 (2019) 503-508.

[10] Tran K.A., Kraus E., Clark A.T., Bennett A., Pogoda K., Cheng X., Cē Bers A., Janmey P.A., Galie P.A.: Dynamic Tuning of Viscoelastic Hydrogels with Carbonyl Iron Microparticles Reveals the Rapid Response of Cells to Three-Dimensional Substrate Mechanics. ACS Applied Materials and Interfaces 13(18) (2021) 20947-20959.

[11] Iacovacci V., Lucarini G., Innocenti C., Comisso N., Dario P., Ricotti L., Menciassi A.: Polydimethylsiloxane Films Doped with NdFeB Powder: Magnetic Characterization and Potential Applications in Biomedical Engineering and Microrobotics. Biomedical Microdevices 17(6) (2015) 112.

[12] Dobson J.: Magnetic Nanoparticles for Drug Delivery. Drug Development Research 67(1) (2006) 55-60.

[13] Yüksel C.: The Use of Neodymium Magnets in Healthcare and Their Effects on Health. Northern Clinics of Istanbul.

[14] Zhou R., Surendran A.N., Mejulu M., Lin Y.: Rapid Microfluidic Mixer Based on Ferrofluid and Integrated Microscale NdFeB-PDMS Magnet. Micromachines 11(1) (2019) 29.

[15] Sitti M., Ceylan H., Hu W., Giltinan J., Turan M., Yim S., Diller E.: Biomedical Applications of Untethered Mobile Milli/Microrobots. Proceedings of the IEEE 103(2) (2015) 205-224.

[16] Peyer K.E., Zhang L., Nelson B.J.: Bio-Inspired Magnetic Swimming Microrobots for Biomedical Applications. Nanoscale 5(4) (2013) 1259-1272.

[17] Saint-Cricq P., Deshayes S., Zink J.I., Kasko A.M.: Magnetic Field Activated Drug Delivery Using Thermodegradable Azo-Functionalised PEG-Coated Core-Shell Mesoporous Silica Nanoparticles. Nanoscale 7(31) (2015) 13168-13172.

[18] Timko B.P., Dvir T., Kohane D.S.: Remotely Triggerable Drug Delivery Systems. Advanced Materials 22 (44) (2010) 4925-4943.

[19] Do V.T., Tang C.Y., Reinhard M., Leckie J.O.: Effects of Chlorine Exposure Conditions on Physiochemical Properties and Performance of a Polyamide Membrane - Mechanisms and Implications. Environmental Science & Technology 46(24) (2012), 13184-13192.

[20] Ducom G., Laubie B., Ohannessian A., Chottier C., Germain P., Chatain V.: Hydrolysis of Polydimethylsiloxane Fluids in Controlled Aqueous Solutions. Water Science and Technology 68(4) (2013) 813-820.

[21] Caulfield M.J., Qiao G.G., Solomon D.H.: Some Aspects of the Properties and Degradation of Polyacrylamides. Chemical Reviews 102(9) (2002) 3067-3084.

[22] Henkelman S., Rakhorst G., Blanton J., van Oeveren W.: Standardization of Incubation Conditions for Hemolysis Testing of Biomaterials. Materials Science and Engineering: C 29(5) (2009) 1650-1654.

[23] Donohue V.E., McDonald F., Evans R.: In Vitro Cytotoxicity Testing of Neodymium-Iron-Boron Magnets. Journal of Applied Biomaterials 6(1) (1995) 69-74.

[24] Evans R.D., McDonald F.: Effect of Corrosion Products (Neodymium Iron Boron) on Oral Fibroblast Proliferation. Journal of Applied Biomaterials 6(3) (1995) 199-202.

[25] Palmer R.J., Butenhoff J.L., Stevens J.B.: Cytotoxicity of the Rare Earth Metals Cerium, Lanthanum, and Neodymium in Vitro: Comparisons with Cadmium in a Pulmonary Macrophage Primary Culture System. Environmental Research 43(1) (1987) 142-156.

[26] Rim K.T., Koo K.H., Park J.S.: Toxicological Evaluations of Rare Earths and Their Health Impacts to Workers: A Literature Review. Safety and Health at Work 4(1) (2013) 12-26.

[27] Ali S., Abdul Rani A.M., Baig Z., Ahmed S.W., Hussain G., Subramaniam K., Hastuty S., Rao T.V.V.L.N.: Biocompatibility and Corrosion Resistance of Metallic Biomaterials. Corrosion Reviews 38(5) (2020) 381-402.

[28] Bakirdere S., Orenay S., Korkmaz M.: Effect of Boron on Human Health. The Open Mineral Processing Journal 3(1) (2010) 54-59.

[29] Nielsen F.H.: Update on Human Health Effects of Boron. Journal of Trace Elements in Medicine and Biology 28(4) (2014) 383-387.

[30] Uthamaraj S., Tefft B.J., Klabusay M., Hlinomaz O., Sandhu G.S., Dragomir-Daescu D.: Design and Validation of a Novel Ferromagnetic Bare Metal Stent Capable of Capturing and Retaining Endothelial Cells. Annals of Biomedical Engineering 42(12) (2014) 2416-2424.

[31] Niemirowicz-Laskowska K., Mystkowska J., Łysik D., Chmielewska S., Tokajuk G., Misztalewska-Turkowicz I., Wilczewska A.Z., Bucki R.: Antimicrobial and Physicochemical Properties of Artificial Saliva Formulations Supplemented with Core-Shell Magnetic Nanoparticles. International Journal of Molecular Sciences 21(6) (2020) 1979.

[32] Leśniewska B., Arciszewska Ż., Wawrzyńczak A., Jarmolińska S., Nowak I., Godlewska-Żyłkiewicz B.: Method Development for Determination of Trace Amounts of Palladium in Environmental Water Samples by ICP-MS/MS after Pre-Concentration on Thiol-Functionalized MCM-41 Materials. Talanta 217 (2020) 121004.

[33] Mystkowska J., Powojska A., Łysik D., Niewęgłowska J., Bermúdez G.S.C., Mystkowski A., Makarov D.: The Effect of Physiological Incubation on the Properties of Elastic Magnetic Composites for Soft Biomedical Sensors. Sensors 21(21) (2021) 7122.

[34] Mystkowska J., Car H. Dąbrowski J.R., Romanowska J., Klekotka M., Milewska A.M.: Artificial Mucin-based Saliva Preparations - Physicochemical and Tribological Properties. Oral Health & Preventive Dentistry 16(2) (2018).

[35] He X., Mu X., Wen Q., Wen Z., Yang J., Hu C., Shi H.: Flexible and Transparent Triboelectric Nanogenerator Based on High Performance Well-Ordered Porous PDMS Dielectric Film. Nano Res. 9 (2016) 3714-3724.

[36] Chuah Y.J., Koh Y.T., Lim K., Menon N.V., Wu Y., Kang Y.: Simple Surface Engineering of Polydimethylsiloxane with Polydopamine for Stabilized Mesenchymal Stem Cell Adhesion and Multipotency. Sci. Rep. 5 (2016) 18162.

[37] Ruben B., Elisa M., Leandro L., Victor M., Gloria G., Marina S., Mian K.S., Pandiyan R., Nadhira L.: Oxygen Plasma Treatments of Polydimethylsiloxane Surfaces: Effect of the Atomic Oxygen on Capillary Flow in the Microchannels. Micro Nano Lett. 12 (2017), 754-757.

MICROSTRUCTURE AND SURFACE FREE ENERGY OF LIGHT-CURED DENTAL COMPOSITES AFTER THEIR MODIFICATION WITH LIQUID RUBBER

Monika Sowa[1] (iD)**, Agata Przekora**[2] (iD)**,
Krzysztof Pałka**[1]* (iD)

[1] Lublin University of Technology,
Faculty of Mechanical Engineering,
Nadbystrzycka 36, 20-618 Lublin, Poland
[2] Medical University of Lublin,
Independent Unit of Tissue Engineering
and Regenerative Medicine,
Chodzki 1, 20-093 Lublin, Poland
*e-mail: k.palka@pollub.pl

Abstract

The use of liquid rubber as a component of light-cured dental composites is one of the methods of increasing their fracture toughness. It also reduces polymerization shrinkage and offers the potential to lower water sorption. The aim of the study was to evaluate the miscibility of liquid rubber in composite matrix resins as well as changes in the wettability and surface free energy (SFE) values of commercial light-curing composites after their modification with liquid rubber. The research materials were Flow Art and Boston (Arkona) light-cured composites and resin mixtures used in their production. Liquid rubber Hypro 2000X168LC VTB (Huntsman Int.) was used as a modifier. The solubility of liquid rubber was assessed under light microscopy. The contact angle and SFE measurements were made on a DSA30 goniometer (Kruss) using water and diiodomethane. It was found that the liquid rubber solubility depended mainly on the viscosity of the resin, which was related to the amount of BisGMA. The resulting mixture showed good temporal stability without larger domains. The curing process released the liquid rubber as a separate phase formed as spherical domains. The morphology of these domains was homogeneous and their size did not exceed 50 µm in diameter. The presence of liquid rubber in modified composites increased their hydrophobicity and reduced the surface free energy value. The obtained properties might help to reduce the formation of bacterial biofilm on dental fillings.

Keywords: dental composite, solubility, liquid rubber, wettability, surface free energy

Introduction

Light-cured polymer-ceramic composites used in dentistry are among the most commonly used biomaterials in the human body. Currently, dental composites account for about 70% of all dental fillings [1]. These materials, made of a polymer matrix reinforced with organic or inorganic mineral or mixed particles of various sizes and shapes, are characterized by good mechanical properties and Young's modulus close to the value of tooth tissue [2]. Since the invention of the BisGMA monomer by Rafael Bowen in 1962, they have become the main direction of development in conservative dentistry, gradually replacing amalgams, silicon cement, and noble metal fillings [3]. The widespread use of composites based on light-curing resins is primarily implied by their good wear resistance, which determines their durability, moreover, the ease of forming and application, or the natural color-matched to the teeth [1].

The properties of dental composites result from their composition. Their matrix is a mixture of methacrylate resins, most often BisGMA, BisEMA, TEGDMA, and UDMA. The size of the reinforcement particle has been reduced over the years until it reached nanometric dimensions to achieve better properties [4]. Apart from changes in the amount and shape of particles and their surface treatment, alterations were also made in the structure or chemistry of the monomer used and the dynamics of the polymerization reaction [5]. Despite many years of development, light-cured dental composites are still not free of disadvantages. Their durability is limited under *in vivo* conditions, which results in a relatively short period of replacement of the filling and causes additional loss of tooth tissue. Despite the improvements, several clinically negative effects of using light-cured composite fillings are still observed, e.g., marginal leakage [6], discolorations [7], cusp fractures [8], unbonding, lack of marginal integrity [9], secondary caries [10,11], postoperative sensitivity or pain [12]. These effects are often associated with polymerization shrinkage stress [9], although there is little clinical evidence to support a clear relationship between these effects [13]. As a result, the above-mentioned disadvantages cause the unwavering interest of the scientific community for medical, technical, and economic reasons.

Research is constantly underway to improve the properties of composites. There are many methods of boosting their mechanical properties, including the use of spherical-shaped reinforcement particles [14], whiskers [15], or glass fibers [16]. Along with the increasing proportion of the ceramic reinforcing phase, a decrease in polymerization shrinkage and an increase in the hardness and strength of these composites were observed, however, most often at the expense of fracture toughness [17]. Reduction of polymerization shrinkage can be achieved, among others, by controlling the proportions of the matrix components [18] and its modification with liquid rubber [19]. The potential increase in the fracture toughness of composites is also possible due to the modification of matrix resins by introducing liquid rubber [20-23]. These modifiers may be, for example, low molecular weight butadiene [24] and butadiene-styrene rubbers [22]. Recent work has also shown an increase in the strength of resins for dental applications due to the use of polybutadiene/bisphenol A copolymers [22]. Poly(butadiene-acrylonitrile-acrylic acid) terpolymer with methacrylate functional groups with good solubility in BisGMA resin caused a 25% increase in fracture toughness and an increase in hydrolytic resistance [21]. This solution uses a copolymer made with the use of acrylic acid, which is, unfortunately, a toxic component also showing a carcinogenic effect [25].

The presence of liquid rubber in the matrix of dental composites, in addition to potentially reducing shrinkage and improving mechanical properties, may also have a positive effect on the hydrophobic and biological properties. Work [26] on bone cement with a modified poly(ethyl methacrylate) matrix with n-butyl(PEMA-nBMA) reinforced with hydroxyapatite showed a reduction in water sorption. In addition, such a modification of the cement matrix reduced the value of the modulus of elasticity and increased its plasticity, which favors the reduction of contact stresses and limits cracking. The hydrophobicity of dental composites enhances protection against hydrolytic degradation [27], bacterial film formation [28], and the resulting biodegradation [29].

This study aims to evaluate the miscibility of liquid rubber in composite matrix resins as well as changes in wettability and the value of surface free energy (SFE) of commercial light-curing composites after their modification with liquid rubber.

Materials and Methods

The variety of dental work requires the use of materials of different viscosities. Therefore, two groups of dental composites were tested: flow type and condensable composites. Commercial light-cured composites Flow-Art (flow type) and Boston (condensable) produced by Arkona Laboratory of Dental Pharmacology in Nasutów were used as control materials. Flow-Art is a micro-hybrid composite consisting of a dimethacrylate organic matrix (BisGMA, UDMA, TEGDMA, EBADMA), reinforced with inorganic particles in the amount of approx. 60% by weight. (barium-aluminum-silicon glass, pyrogenic silica) and additional substances (photoinitiator, co-initiator, inhibitor, stabilizers, pigments). Boston is a micro-hybrid light-cured composite. Its matrix is the same mixture of resins as in the case of Flow-Art but with different proportions of components, thanks to which this resin has a lower viscosity, and therefore it is optimized for mixing with a higher amount of reinforcement. The reinforcement of the Boston composite consists of 78 wt% barium-aluminum-silica glass and pyrogenic silica. The composition of the above-mentioned commercial composites is proprietary by the manufacturer and, for confidentiality reasons, it is not presented in detail here.

All composites were made by Arkona based on Polish patent no. 238167.

The research material consisted of analogous composites (flow and condensable type), in which the matrix resin was modified with liquid rubber in an amount of 5% by weight to the resin. Synthetic nitrile-free polybutadiene rubber Hypro 2000X168LC VTB (CAS 68649-04-7; Huntsman International LLC, USA) was used [30]. The liquid rubber was characterized by a relatively light color (4 on the Gardner scale), which did not affect the shade of the final product. The following samples marks were used:
- F – Flow Art composite,
- FM – Flow Art composite modified with liquid rubber,
- B – Boston composite
- BM – Boston composite modified with liquid rubber

For the miscibility tests, resin blends used in commercial Flow-Art and Boston materials containing a package of additional ingredients (initiator, stabilizer, inhibitor) were used. The following resin designations were used:
- resin F - the resin used in the Flow-Art composite, and
- resin B - used in the Boston composite.

The viscosities of these resins, determined at 23°C, were 12 Pa·s for resin F and 7 Pa·s for resin B. The portions of the resins were mechanically mixed with the rubber in predetermined weight proportions in a darkened room, preventing the material from curing. Evaluation of the miscibility and stability of the mixture was performed with a light microscope (Eclipse MA200, Nikon, Japan). Undissolved liquid rubber formed a separate phase in the liquid resin mixture. The samples were placed on a microscopic glass slide with spacers at the edges to ensure a resin layer thickness of 20 µm. Having covered the slide with the applied sample with a coverslip, the desired thickness of the specimen was obtained. Observations were made in the yellow-transmitted light. The first images were taken immediately after mixing the resin with the rubber, while the next images after 1 and 24 h, securing the material against curing. The final images were taken after curing with a LED lamp with an intensity of 1400 mW/cm^2 for 20 s (Cromalux LED 1200, Mega-PHYSIK GmbH & Co., Germany). After curing, the presence of the second phase was also observed.

The composite samples for the contact angle Θ and surface free energy (SFE) γ_S measurements were prepared as discs of 15 mm in diameter and 1 mm in height according to the ISO 4049 standard. The measurements mentioned above were carried out using the sessile drop technique on a DSA30 goniometer (Kruss, Germany) using type I ultrapure water (obtained from Milli-Q® system, Merck Millipore) and diiodomethane (Sigma Aldrich Chemicals) as polar and non-polar liquid, respectively. The liquid droplets were dosed at 2 µL. The samples were tested 24 h after polymerization (dry stored) as well as after 24 h incubation in distilled water as simulations of the oral environment to evaluate changes in surface properties under the influence of the aqueous environment. Surface free energy and its components, polar γ_S^P and dispersion γ_S^D, were determined based on the Owens-Wendt method [31]. For each type of the material, four samples were prepared and at least five measurements were taken (N > 20).

The results were assessed for statistically significant differences between the mean values using the Student's t-test for independent samples, with the Statistica software (TIBCO Software Inc.) at the significance level α <0.05.

Results and Discussions

The microscopic observation of the resins without modification showed their complete homogeneity, with no inclusions or foreign phases present. The curing process did not change the morphology of these resins either.

The effects of mixing resins with liquid rubber and their time stability are shown in FIG. 1. The components formed a homogeneous system immediately after mixing. Over time, spherical domains of rubber with diameters ranging from less than 1 µm to approx. 10 µm were released from the system. For resin B (with lower viscosity), rubber dissolution was initially observed, followed by the release of domains. Additional studies revealed that the solubility limit of liquid rubber in this resin was about 4%. After the liquid rubber was mixed with resin F, which was characterized by a higher viscosity, the domains of a slightly larger size than those released in resin B were observed. After 24 h in resin F, the formation of larger domains was observed by joining the smaller precipitates. In both resins, the morphology of the liquid rubber showed a homogeneous distribution over the entire volume.
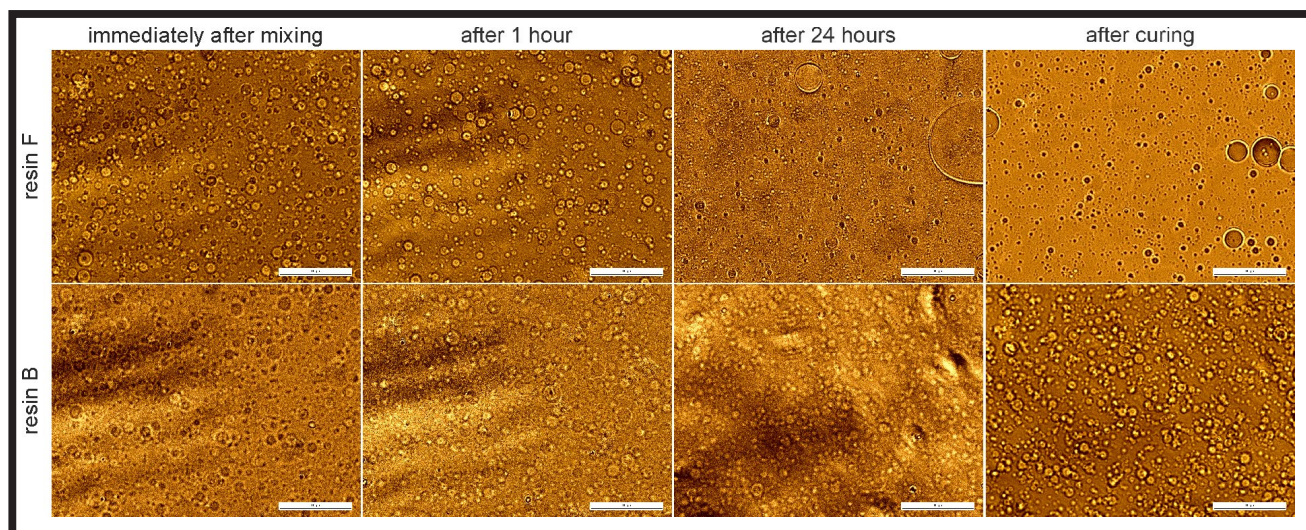
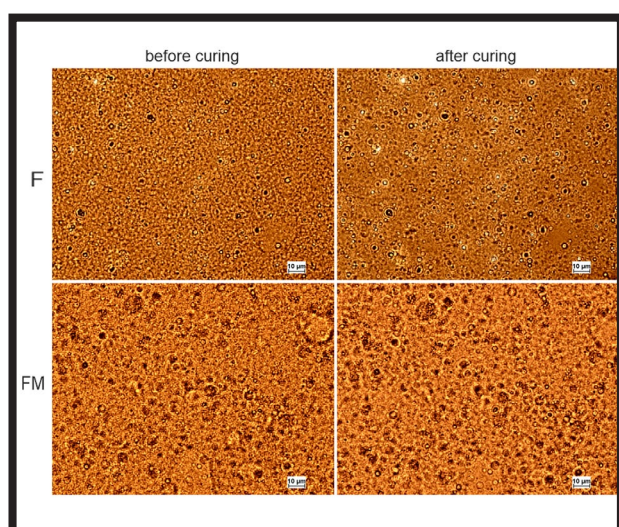**FIG. 1. Solubility and morphology of liquid rubber domains in the tested resins (scale bars 100 μm).**

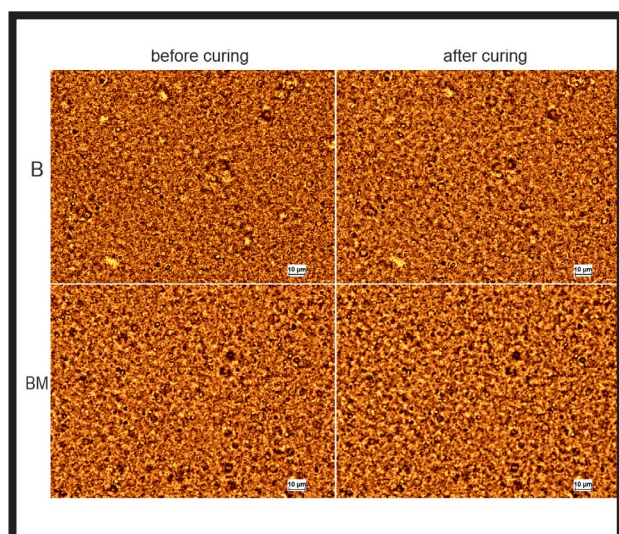**FIG. 2. Microstructures of F and FM composites before and after curing.**

FIG. 3. Microstructures of B and BM composites before and after curing.

The mixture of liquid rubber in the resins, especially those with higher viscosity, did not show satisfactory stability as the domains of large size were formed. It was observed in two-component systems (resin - liquid rubber), while in multicomponent systems (resin - liquid rubber - ceramic particles) higher stability was noted, as a result of higher size reduction of the domains due to mixing and blocking their movement in the presence of particles.

The microstructure of flow-type composites before and after polymerization is shown in FIG. 2. In the case of a composite without modification, fine reinforcement particles were visible, including translucent ceramic particles visible due to illumination. The material microstructure was homogeneous, the reinforcement was evenly distributed without clusters or agglomerates. Polymerization did not change the appearance of the microstructure. The composites after modification with liquid rubber also showed homogeneous structure without the clusters of reinforcement particles. However, after the modification, the composite microstructure changed, i.e. a large number of round (probably spherical) domains (marked with arrows in the figure) with a diameter of approx. 1-2 μm appeared.

The reinforcement particles located inside the domains were also observed as a result of good wetting and compatibility of liquid rubber with silica reinforcement [30]. The curing process caused the formation of "shells" resulting from a change in optical properties, as well as possible deformation of the rubber due to the polymerization shrinkage of the resin. Comparing the domains before and after curing, it could be stated that there were no noticeable differences in their sizes, yet their optical properties changed - after curing they were much darker. In some areas, the domains were not visible before curing. However, after curing, round rubber domains were revealed due to the release of the second phase or the domains being pushed out of the deeper layers of the composite, in consequence of viscosity changes during curing or polymerization shrinkage.

The microstructure of the condensable composite B (FIG. 3) showed high uniformity of ceramic phase dispersion; there were no clusters and agglomerates. Larger particles as brighter spots were visible. The curing process, similarly to the case of composite F, did not significantly change the appearance of the microstructure. In composite B, there were also visible "shells" formed around the reinforcement particles, caused by changes in the optical properties of the resin due to the generated stresses and polymerization shrinkage, and changes in the resin viscosity during polymerization.

Images of liquid drops on the surface of tested materials, which were the basis for the measurement of the contact angle and SFE, are shown in FIG. 4, and after the 24 h incubation in water, in FIG. 5.

The results of the contact angle measurements together with the value of the surface free energy and its components: dispersion and polar, are presented in TABLE 1 and FIG. 6.

The results of the measurement of contact angles for composite surfaces were consistent with those obtained by Rüttermann S. et al. [32]. All the tested materials showed hydrophilic surface properties ($\Theta < 90°$ [19]). Modification of both types of composites significantly increased the water's contact angle, but it still remained at a level below 90°. The reasons for the hydrophobicity increase of the rubber-modified composites should be seen in the change of surface topography (increased roughness), as well as in physicochemical factors. Bis-GMA resin, as the main component of the composite' matrix, has polar hydroxyl groups [33], while liquid rubber is non-polar [34], which will increase the contact angle.

Following the presumptions contained in the article [35] it was found that the increase in the micro-roughness of the composites surface after modification may result from a different morphology of the reinforcement in the matrix due to the presence of liquid rubber whose properties are different from the properties of the rest of the resin matrix. Nanosized particles may preferentially be placed in the rubber domains, thus causing changes in the micro-roughness. Such a location of the reinforcement particles in the rubber domains was confirmed by additional microscopic observations (not presented here).

After the incubation, a statistically significant reduction in the water's contact angle value was observed for the FM material, while the BM became significantly more hydrophobic. Lower values of contact angles after incubation in water indicated an increase in hydrophilicity, which might be related to the formation of bridged hydrogen bonds between the absorbed water and the composite surface [32].
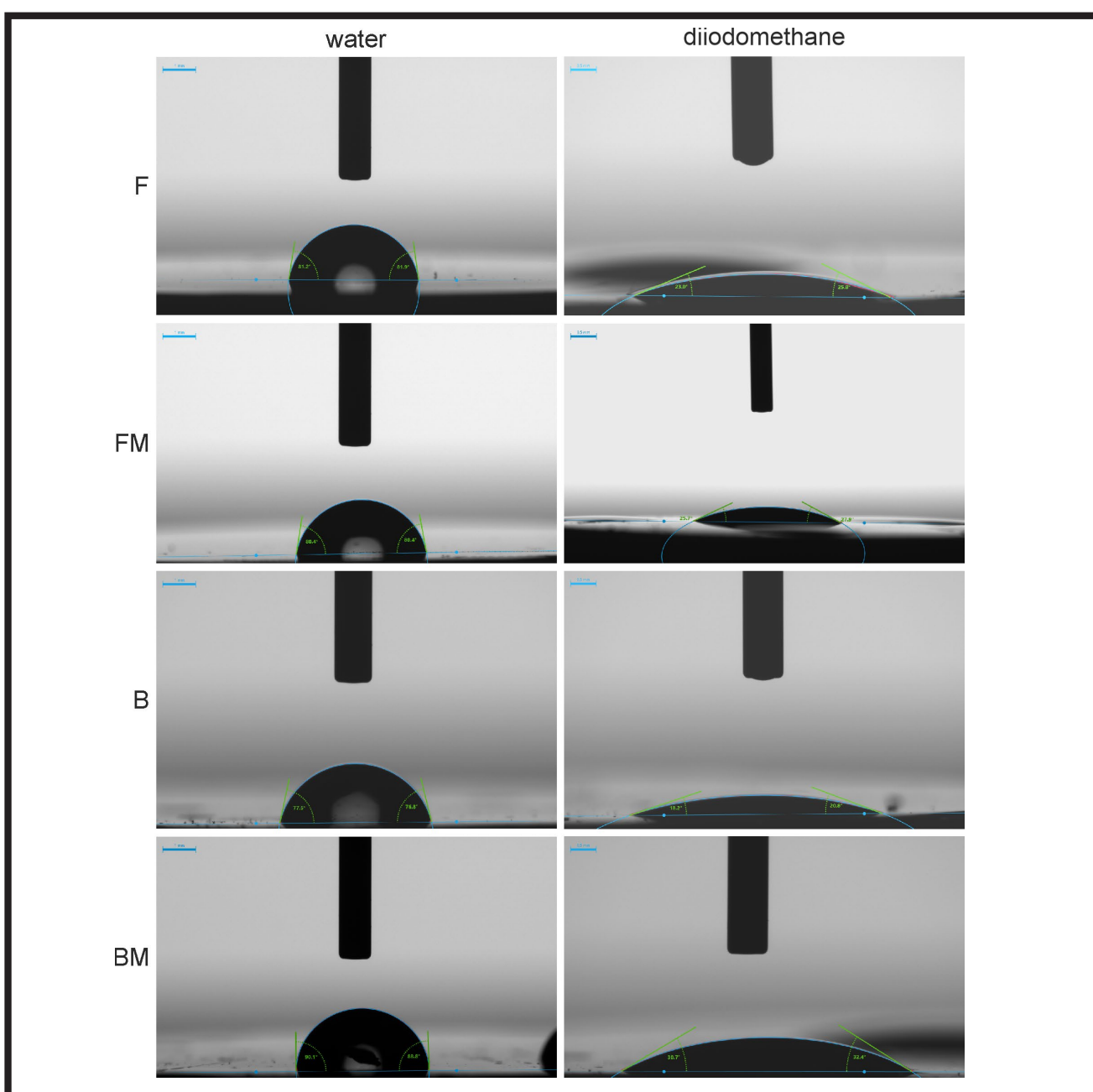

FIG. 4. Representative images of liquid droplets on the surfaces of the tested materials after curing.
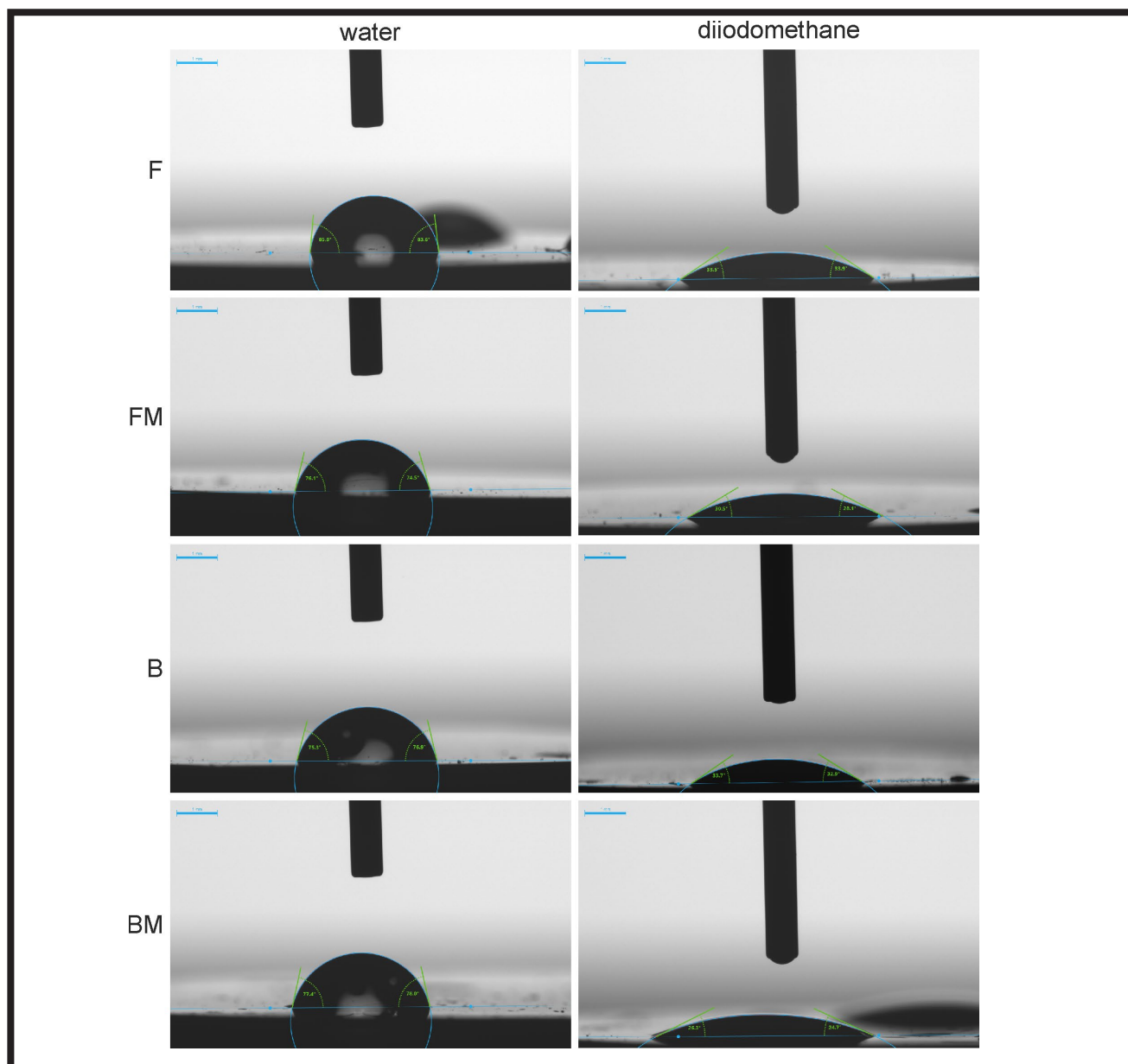
FIG. 5. Representative images of liquid droplets on the surfaces of tested materials after curing and 24 h of incubation in distilled water.

TABLE 1. Summary of the measurement results of the contact angle and surface free energy of the tested composites immediately after polymerization and after 24 h incubation in distilled water. The indices at the Θ angles for water and SFE mean statistically significant differences between the determined values.

Composites	F	FM	B	BM
after curing				
contact angle (water) Θ [deg]	78.62 ± 2.48 [1]	81.98 ± 2.74 [1,2]	75.39 ± 1.51 [3]	77.23 ± 1.92 [3,4]
contact angle (diiodomethane) Θ [deg]	23.55 ± 1.64	23.68 ± 3.15	25.26 ± 2.20	20.08 ± 1.24
Dispersive component of surface energy [mJ/m^2]	46.66 ± 0.56	46.61 ± 1.07	47.76 ± 0.37	46.06 ± 1.27
Polar component of surface energy [mJ/m^2]	2.68 ± 0.71	1.81 ± 0.66	2.91 ± 0.57	3.79 ± 0.53
SFE [mJ/m^2]	**49.33 ± 1.27 [a]**	**48.42 ± 1.74**	**50.67 ± 0.94 [c]**	**49.84 ± 1.74 [e]**
after 24 h of incubation In distilled water				
contact angle (water) Θ [deg]	78.24 ± 4.68	78.17 ± 2.10 [2]	75.44 ± 2.32 [3,5]	83.77 ± 3.05 [4,5]
contact angle (diiodomethane) Θ [deg]	33.34 ± 2.54	28.48 ± 2.37	29.97 ± 3.07	27.78 ± 2.69
Dispersive component of surface energy [mJ/m^2]	42.78 ± 1.14	44.84 ± 0.94	44.23 ± 0.79	45.12 ± 1.05
Polar component of surface energy [mJ/m^2]	3.46 ± 1.53	3.11 ± 0.66	4.12 ± 0.85	1.58 ± 0.69
SFE [mJ/m^2]	**46.24 ± 1.67 [a,b]**	**47.95 ± 1.61 [b]**	**48.36 ± 1.12 [c,d]**	**46.70 ± 1.32 [d,e]**
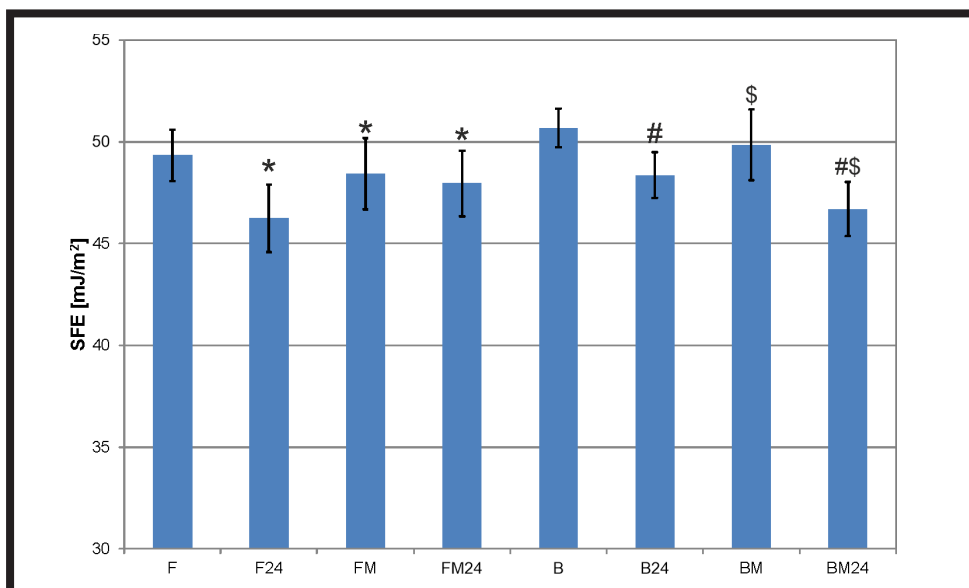
FIG. 6. Summary of SFE measurement results for materials without and after 24 h of incubation in distilled water (the number 24 in the sample designation). The symbols (*) indicate statistically significant differences against material F, (#) - against material B, $ - statistically significant difference between materials BM and BM24.

Higher contact angles might be associated with the existence of strong repulsive forces between the surface and the absorbed water molecules. This could create a thin and even more hydrophobic layer above the surface of the water-saturated material. This layer might be a surface that can be damaged by abrasion but also renewed during the service life of the filling.

The values of the surface free energy γ_s for the tested materials before and after incubation in water, along with the statistically significant differences, are presented in FIG. 6. A statistically significant decrease in the SFE value was noted in the case of composite FM when comparing to F, from 49.33 to 48.42 mJ/m². Composite B achieved a higher SFE value compared to F composite, however, similar to BM and FM composites, which indicated the effect of a higher amount of reinforcement. Composite BM showed lower values of SFE than the composite B ones, yet the differences did not show statistical significance. The incubation in water significantly lowered the surface free energy values for all the tested materials. Importantly, in all the tested composites, the dispersion component has a decisive share in the surface free energy value, which means a higher adhesive affinity for non-polar substances. Similar dependencies were revealed by Rüttermann et al. [32]. For FM composite, the value of this component decreased by 32% compared to the F one. On the other hand, an increase in the polar component value was achieved for BM composite.

The obtained results of γ_s presented higher values than those reported in the studies [32,36]. An increase in surface free energy was related to a different composition of resins and reinforcement; it might also suggest the adhesion reduction resulting in a limited formation of a bacterial film.

An increase in the wettability or free energy of the surface of dental fillings is an important factor contributing to the plaque formation on dental materials [37]. Many studies on dental composites wettability indicated that hydrophobic surfaces have a lower potential for bacterial colonization [38]. Thus, the materials for dental fillings should have good wettability to the bonding system to ensure the required adhesion of the joint, while the outer surface should show low wettability to prevent bacterial adhesion.

Thus, the modification of dental composites with liquid rubber favored their hydrophobicity and lowered the surface free energy value. It is particularly important in terms of reducing the possibility of colonization of such modified fillings by bacteria.

Conclusions

The miscibility of Hypro 2000X168LC liquid rubber with the blend of methacrylate resins was limited by their composition and viscosity. However, regardless of miscibility, the curing process released the liquid rubber as a separate phase in the form of spherical domains. The morphology of these domains was homogeneous, and their size did not exceed 50 µm in diameter.

The presence of liquid rubber in modified composites increased their hydrophobicity and reduced the value of surface free energy. The obtained properties might reduce the formation of bacterial biofilm on the dental fillings, while the adhesion to the bonding system might strengthen the bond between the filling and the tooth tissues. A tendency to limit water sorption as a result of liquid rubber modification was also observed.

Acknowledgements

ORCID iD

M. Sowa: https://orcid.org/0000-0001-5784-3701
A. Przekora: https://orcid.org/0000-0002-6076-1309
K. Pałka: https://orcid.org/0000-0003-4920-4613

References

[1] Bociong K., Krasowski M., Domarecka M., Sokołowski J.: Wpływ metody fotopolimeryzacji kompozytów stomatologicznych na bazie żywic dimetakrylanowych na naprężenia skurczowe oraz wybrane właściwości utwardzonego materiału. Polimery/Polymers 61 (2016) 499-508.

[2] Pawłowska E., Loba K., Błasiak J., Szczepańska J.: Właściwości i ryzyko stosowania metakrylanu bisfenolu a i dimetakrylanu uretanu - podstawowych monomerów kompozytów stomatologicznych. Dent. Med. Probl. 46 (2009) 477-485.

[3] Schmidseder J., Stomatologia Estetyczna. Wydawnictwo Czelej 2011.

[4] Garoushi S., Lassila L.V.J., Vallittu P.K.: Influence of nanometer scale particulate fillers on some properties of microfilled composite resin. J. Mater. Sci. Mater. Med. 22 (2011) 1645-1651.

[5] Ferracane J.L.: Current trends in dental composites. Crit. Rev. Oral Biol. Med. 6 (1995) 302-318.

[6] Braga R. R., Hilton T.J., Ferracane J.L.: Contraction stress of flowable composite materials and their efficacy as stress-relieving layers. J. Am. Dent. Assoc. 134 (2003) 721-728.

[7] Priyalakshmi S., Ranjan M.: A Review on Marginal Deterioration of Composite Restoration. IOSR J. Dent. Med. Sci. 13 (2014) 06-09.

[8] Fennis W.M.M., Kuijs R.H., Kreulen C.M., Roeters F.J.M., Creugers N.H.J., Burgersdijk R.C.W.: A survey of cusp fractures in a population of general dental practices. Int. J. Prosthodont. 15 (2002) 559-63.

[9] Ferracane J.L., Mitchem J.C.: Relationship between composite contraction stress and leakage in Class V cavities. Am. J. Dent. 16 (2003) 239-243.

[10] Ferracane J.L.: Models of Caries Formation around Dental Composite Restorations. J. Dent. Res. 96 (2017) 364-371.

[11] Kuper N.K., Van De Sande F.H., Opdam N.J.M., Bronkhorst E.M., De Soet J.J., Cenci M.S., Huysmans M.C.D.J.N.M.: Restoration materials and secondary caries using an in vitro biofilm model. J. Dent. Res. 94 (2015) 62-68.

[12] Celerino I.C.C.M.: Post-operative sensitivity in direct resin composite restorations: Clinical practice guidelines. Int. J. Res. Discov. 1 (2012) 1-12.

[13] Ilie N., Hickel R.: Resin composite restorative materials. Aust. Dent. J. 56 (2011) 59-66.

[14] Kim K., Ong J., Okuno O.: The effect of filler loading and morphology on the mechanical properties of contemporary composites. J. Prosthet. Dent. 87 (1992) 642-649.

[15] Xu H.H.K., Quinn J.B., Smith D.T., Giuseppetti A.A., Eichmiller F.C.: Effects of different whiskers on the reinforcement of dental resin composites. Dent. Mater. 19 (2003) 359-367.

[16] Elbishari H., Satterthwaite J., Silikas N.: Effect of filler size and temperature on packing stress and viscosity of resin-composites. Int. J. Mol. Sci. 12 (2011) 5330-5338.

[17] Xu H.H.K.: Dental composite resins containing silica-fused ceramic single-crystalline whiskers with various filler levels. J. Dent. Res. 78 (1999) 1304-1311.

[18] Pałka K., Janiczuk P., Kleczewska J.: Polymerization shrinkage of resin mixtures used in dental composites. Eng. Biomater. 154 (2020) 16-21.

[19] Pałka K.: Polymerization Shrinkage of New Dental Composites Modified With Liquid Rubber. Eng. Biomater. 158 (2020) 19.

[20] Lee V.A., Cardenas H.L., Rawls H.R.: Rubber-toughening of dimethacrylate dental composite resin. J. Biomed. Mater. Res. - Part B Appl. Biomater. 94 (2010) 447-454.

[21] Kerby R.E., Tiba A., Knobloch L.A., Schricker S.R., Tiba O.: Fracture toughness of modified dental resin systems. J. Oral Rehabil. 30 (2003) 780-784.

[22] Matsukawa S., Hayakawa T., Nemoto K.: Development of high-toughness resin for dental applications. Dent. Mater. 10 (1994) 343-346.

[23] Palka K., Kleczewska J., Sasimowski E., Belcarz A., Przekora A.: Improved fracture toughness and conversion degree of resin-based dental composites after modification with liquid rubber. Materials (Basel) 13 (2020) 1-13.

[24] Rodford R.A.: Further development and evaluation of high impact strength denture base materials. J. Dent. 18 (1990) 151-157.

[25] Dusek K., Lednicky F., Lunak S., Mach M., Duskova D.: Toughening of Epoxy Resins With Reactive Polybutadienes., in: Riew C.K., Gillham J.K. (Eds.), Advances in Chemistry Series. Advances in Chemistry (1984) 27-35.

[26] Deb S., Braden M., Bonfield W.: Water absorption characteristics of modified hydroxyapatite bone cements. Biomaterials 16 (1995) 1095-1100.

[27] Sadek F.T., Castellan C.S., Braga R.R., Mai S., Tjäderhane L., Pashley D.H., Tay F.R.: One-year stability of resin-dentin bonds created with a hydrophobic ethanol-wet bonding technique. Dent. Mater. 26 (2010) 380-386.

[28] Pałka K., Miazga-Karska M., Pawłat J., Kleczewska J., Przekora A.: The effect of liquid rubber addition on the physicochemical properties, cytotoxicity and ability to inhibit biofilm formation of dental composites. Materials (Basel) 14 (2021) 1704.

[29] Moussa D.G., Fok A., Aparicio C.: Hydrophobic and antimicrobial dentin: A peptide-based 2-tier protective system for dental resin composite restorations. Acta Biomater. 88 (2019) 251-265.

[30] CVC Thermoset Specialties, Hypro ® 2000X168LC VTB. Technical Bulletin. 2019.

[31] Rudawska A., Jacniacka E.: Analysis for determining surface free energy uncertainty by the Owen-Wendt method. Int. J. Adhes. Adhes. 29 (2009) 451-457.

[32] Rüttermann S., Trellenkamp T., Bergmann N., Raab W.H.M., Ritter H., Janda R.: A new approach to influence contact angle and surface free energy of resin-based dental restorative materials. Acta Biomater. 7 (2011) 1160-1165.

[33] Cornelio R.B., Wikant A., Mjosund H., Kopperud H.M., Haasum J., Gedde U.W., Örtengren U.T.: The influence of bis-EMA vs bis GMA on the degree of conversion and water susceptibility of experimental composite materials. Acta Odontol. Scand. 72 (2014) 440-447.

[34] Xu S.A.: Miscibility and Phase Separation of Epoxy/Rubber Blends, in: Parameswaranpillai J., Hameed N., Pionteck J., Woo E.M. (Eds.), Handbook of Epoxy Blends. Springer International Publishing AG (2017) 68-100.

[35] Sumita M., Sakata K., Asai S., Miyasaka K., Nakagawa H., Dispersion of fillers and the electrical conductivity of polymer blends filled with carbon black. Polym. Bull. 25 (1991) 265-271.

[36] Namen F.M., Ferrandini E., Galan J.: Surface energy and wettability of polymers light-cured by two different systems. J. Appl. Oral Sci. 19 (2011) 517-520.

[37] Ono M., Nikaido T., Iked M., Imai S., Hanada N., Tagami J., Matin K.: Surface properties of resin composite materials relative to biofilm formation. Dent. Mater. J. 26 (2007) 613-622.

[38] Gyo M., Nikaido T., Okada K., Yamauchi J., Tagami J., Matin K.: Surface response of fluorine polymer-incorporated resin composites to cariogenic biofilm adherence. Appl. Environ. Microbiol. 74 (2008) 1428-1435.

FISH COLLAGEN AND CHITOSAN MIXTURES AS A PROMISING BIOMATERIAL FOR POTENTIAL USE IN MEDICINE AND COSMETIC INDUSTRY

Alina Sionkowska[1]*, **Katarzyna Musiał**[1], **Magdalena Gadomska**[1], **Katarzyna Adamiak**[2]

[1] Department of Chemistry of Biomaterials and Cosmetics, Nicolaus Copernicus University in Toruń, Gagarina 7, 87-100 Toruń, Poland
[2] WellU, Sp. z o.o., Wielkopolska 280, 81-531 Gdynia, Poland
*e-mail: alinas@umk.pl

Abstract

For the last three decades, an increasing interest in new materials based on blends of two or more polymers has been observed. Fish skin collagen and chitosan are constantly highly popular among scientists. This study aimed to obtain thin films from mixtures of low and medium molecular weight chitosan with fish collagen in three different ratios and examine their features for potential use in medicine and cosmetic industry. Polymer blends in ratios 25:75, 50:50, and 75:25 were made to obtain thin films. The infrared spectroscopy, mechanical properties study, contact angle measurements, topographic imaging, and swelling test were used to characterize the features of the films. A statistical appraisal of the results was conducted with the Q-Dixon's test. The infrared spectroscopy analysis showed that in the IR spectra of the examined biomaterials, there are shifts in the bands positions proving intermolecular interactions between collagen and chitosan in the blends. The mechanical properties in the mixtures were different from those of a single biopolymer film. Hydrophilicity and polarity of the blends decrease with the increasing collagen content, which may suggest that the adhesion to the skin will be enhanced. The surface topography of the obtained films varies depending on the ratio of biopolymers in the mixtures. The swelling tests indicated that chitosan absorbs more water than collagen. The properties of the films made of collagen-chitosan mixtures vary depending on the molecular weight of chitosan and the content of each biopolymer in the blend.

Keywords: *collagen, chitosan, biomaterials, blends, medicine, cosmetics*

Introduction

Chitosan is a cationic copolymer obtained by the chitin alkaline deacetylation process. It is constructed of 2-amino-2-deoxy-D-glucopyranose units, which are mostly devoid of acetyl groups and connected with a β-1,4-glycosidic bond [1,2]. Chitosan is present in some fungi species' cell walls but its content is much lower than in the case of chitin [3]. In the medical and cosmetic industries such properties of chitosan as biodegradability, biocompatibility, non-toxicity, mucoadhesiveness, anti-tumor, and antibacterial activity are the most desired. The possibility of processing chitosan in many different forms, such as thin films, membranes, nanoparticles, hydrogels, and scaffolds, is also of significance.

Collagen is the most abundant protein in the human body, where it plays an important role in providing the strength and right structure maintenance of the tissues and creating a scaffold for internal organs [4-6]. Currently, 29 types of genetically different collagen are known [7]. In the human body, type I, II, and III are primarily found [4]. Due to the risk of typical hoggery and cattle zoonotic diseases transmission, as well as religious aspects, the interest in the alternative for mammalian collagen increased [8,9]. The attention focused on fish waste which makes up about 50-70% of the seafood production [9,10]. In favor of using fish for collagen production speaks the 75% content of this protein in a fish body. Skin, head, scales, bones, fins, air bladders, and other entrails can be used in the extraction process of this biopolymer [11]. Due to the lower hydroxyproline content, fish collagen is marked by a significantly lower denaturation temperature in comparison to mammalian collagen. In this regard, collagen extracted from silver carp (Hypophthalmichthys molitrix) stands out. It shows quite a high denaturation temperature in contrast with other fish species [10,12].

Compared to their pure components, mixtures of chitosan and collagen gain unique mechanical and structural properties [13]. The materials obtained from the mentioned blends are bioresorbable, elastic, amenable to further modifications, and have higher resistance to enzymes than pure collagen [14]. The fact that after combining both biopolymers there is still a possibility to obtain different forms such as thin films, membranes, hydrogels, and sponges is also an eminent advantage. All of these features make collagen-chitosan mixtures, as well as the polymers that create them, widely applicable in the medicine and cosmetic industries [7].

Chitosan and collagen blends can mimic the extracellular matrix to a large extent, thus contributing to the growth and proliferation of cells. These properties are used in dermal matrixes production, which are applied for treating full-depth wounds [15]. The influence of the mixtures on matrix mineralization as well as on proliferation and differentiation of osteoblasts finds its use in artificial bones and bone tissue implants production [7]. Chitosan-collagen crossed-linked membranes can be used successfully for artificial cornea fabrication and other tissue engineering purposes [16]. Crosslinking of scaffolds made of mentioned biopolymers makes it possible to use them in cartilage regeneration and reconstruction [17]. The medicine also benefits from chitosan-collagen scaffolds made by the 3D-printing method, which are able to partially recreate the right environment for axons regeneration. This feature is used in the spinal cord injury treatment [18]. By crosslinking chitosan-collagen microspheres obtained in the emulsification process, it is possible to use them in the increasingly popular cytotherapy. These microspheres form a matrix for the 3D macrophage proliferation. The studies indicated that such microspheres increased the proliferation, lifetime, and functionality of the macrophages [19].

For the cosmetic industry, the mechanical properties, the surface roughness and wettability of polymeric thin films are significant. It is possible to adjust these features by combining collagen and chitosan in different ratios [11]. The film forming properties of the mentioned biopolymers make both of them valuable ingredients for various kinds of cosmetics. They create a thin layer on the skin surface and limit transepidermal water loss, which contributes to better hydration of the epidermis [11]. The chitosan-collagen blend with an addition of hyaluronic acid can make a valuable component of haircare products [20]. Collagen in the form of peptides is used for stimulating the production of this protein in the skin, protecting skin lipids from degradation and preventing photoaging [21,22]. Chitosan-collagen hydrogels can be loaded with vitamins, antioxidants, or other active ingredients, making up the base for various kinds of cosmetic products and reducing the use of preservatives thanks to the antibacterial properties of chitosan [23]. Collagen peptide nanoparticles and chitosan nanoparticles can be used as emulsion stabilizers. The studies showed that emulsions with the addition of the mentioned stabilizer were marked by very high stability during storage [24]. Chitosan-collagen composites in the presence of proper additives are used for making 3D models of the human skin. It is an increasingly used alternative for testing new active substances on animals. Such components also enable the determination of the efficacy of a given ingredient and its potential to cause phototoxic reactions [25].

In this work, the blends of collagen from skin of Silver carp and chitosan were prepared, and their properties were studied. To the best of our knowledge such blends have not been studied yet.

Materials and Methods

Collagen (Col) from the skins of Silver carp (Hypophthalmichthys molitrix) was purchased from WellU Sp. z o.o., Gdynia, Poland. Low molecular weight chitosan (LCh) and medium molecular weight chitosan (MCh) were purchased from Sigma-Aldrich, Iceland. Sodium chloride was purchased from STANLAB, Poland. 99.5%-99.9% acetic acid and glycerine were purchased from CZDA – POCH, Poland. A 0.5M acetic acid solution was prepared by diluting a concentrated acetic acid with distilled water. To obtain the 2% solutions of collagen and both types of chitosan, each biopolymer was dissolved in the previously prepared solvent, which is 0.5M acetic acid. Mixtures of the previously prepared polymeric solutions were made by combining them in three different ratios: 25:75, 50:50, and 75:25. Thin films were obtained by pouring 25 g of each solution onto plastic plates measuring 100x100x20 mm. To investigate the films properties, the following equipment was used: Thermo Fisher SCIENTIFIC PIKE GladiATR NICOLET iS10, Waltham, MA, USA for obtaining IR spectra and OMNIC 9 software to edit the spectra; Zwick/Roell Z 0.5 testing machine, Ulm, Germany for the mechanical properties analysis; goniometer with a system of drop shape analysis (DSA 10, Krüss, Germany for the contact angle measurement; Multimode scanning probe microscope with a Nanoscope IIIa controller (Veeco Digital Instruments, Santa Barbara, CA, USA) working in air atmosphere, room temperature and tapping mode for the topographic imaging and NanoScope Analysis 1.40 software for editing the images. Using the contact angle measurements, the values of surface free energy were calculated by the Owens-Wendt method. A swelling test of the film samples in a PBS buffer solution with a pH of 7.4 was done. The statistical appraisal of the results was conducted with the Q-Dixon's test. All photographs were taken by one of the authors with a POCO X3 Pro smartphone camera.

Results and Discussions

Obtaining biopolymeric films

Photographs of the obtained polymeric films are presented in FIG. 1. The fish collagen film is translucent and mat (FIG. 1a). The chitosan films are clear and glossy (FIGs. 1b, 1f). The films made of chitosan-collagen blends are mat, the higher the collagen content is, the more opaque they are (FIGs. 1c-e, FIGs. 1g-i).

FTIR spectroscopy analysis

For each obtained film, Infrared spectroscopy analysis was done. The IR spectra of examined biomaterials are shown in FIG. 2.

FIG. 2a shows that the FTIR spectra of LCh and MCh are almost the same. The analysis revealed that the amide I peak observed in fish collagen at 1631 cm^{-1} is present in the chitosan spectra at 1640 cm^{-1} in LCh and 1636 cm^{-1} in MCh. The amide II peak appears at 1544 cm^{-1} in the collagen spectra and 1556 cm^{-1} in the chitosan spectra. The amide III peak characteristic for collagen disappears in the spectra of chitosan. In the range between 2000 cm^{-1} and 4000 cm^{-1}, chitosan shows a greater absorbance than collagen.

The analysis indicated that in the IR spectra of the blends (FIGs. 2b-g) the amide A and amide I peaks are shifted in comparison to the corresponding peaks in the pure polymers spectra. The amide B peaks are in the same position as in the chitosan spectra.

The amide II peak in the blend with the 75% MCh content (FIG. 2e) does not change its position in regard to the same peak in the pure collagen spectra. As for the same blend with LCh instead (FIG. 2b), shifts are present regarding the collagen, and LCh spectra. In the remaining blends with LCh (FIG. 2c, 2d) the amide II peak position is consistent with its position in the pure LCh spectra.

In the 75:25 (FIG. 2e) and 50:50 MCh-Col blends (FIG. 2f), there is no peak of the CH$_2$ group present in the fish collagen spectra. Only in the 25:75 MCh-Col blend (FIG. 2g), the CH$_2$ peak appears without a significant shift. As for the LCh-Col blends, the shifted CH$_2$ peak is present when the LCh content comes to 25% (FIG. 2d) and 50% (FIG. 2c). In all of the blends, the CH$_2$ peak does not change its position with regard to the pure LCh, and MCh blends spectra.

The amide III peak appears in the blends spectra at the higher wavelength number; the higher the chitosan content in the given mixture is. At the 75% collagen content (FIGs. 2d, 2g) the amide III peak has a position similar to that in the pure collagen spectra.

The C-O-C group peaks present in the chitosan spectra do not exist in the pure collagen spectra due to the absence of a glycosidic bond in this protein's structure. The C-O-C peaks appear in all the blends spectra without significant shifts, except the blends with a 25% LCh and MCh content, where the peak at 1071 cm^{-1} is shifted and the blend with a 75% LCh content, where the 1029 cm^{-1} is shifted.

The changes observed in the peaks positions are indicative of interactions between fish collagen and chitosan as well as of good miscibility of the mentioned polymers in each studied ratio. The effect of these interactions is the formation of new hydrogen bonds between the carboxylic, amine, and hydroxyl groups present in the studied biopolymers. Furthermore, in the blends, ionic interactions might appear between protonated amine groups of chitosan and anionic groups of the collagen.
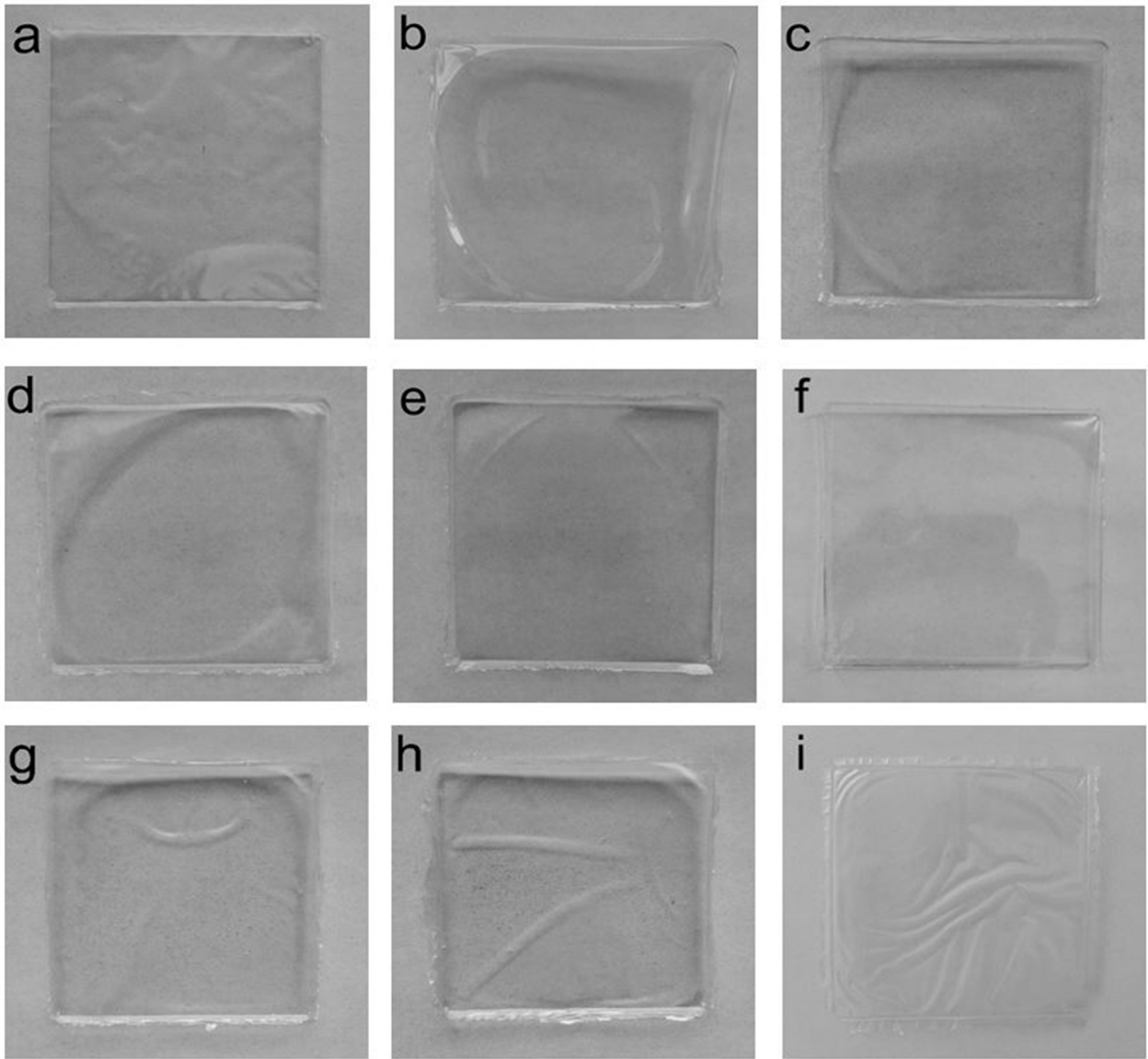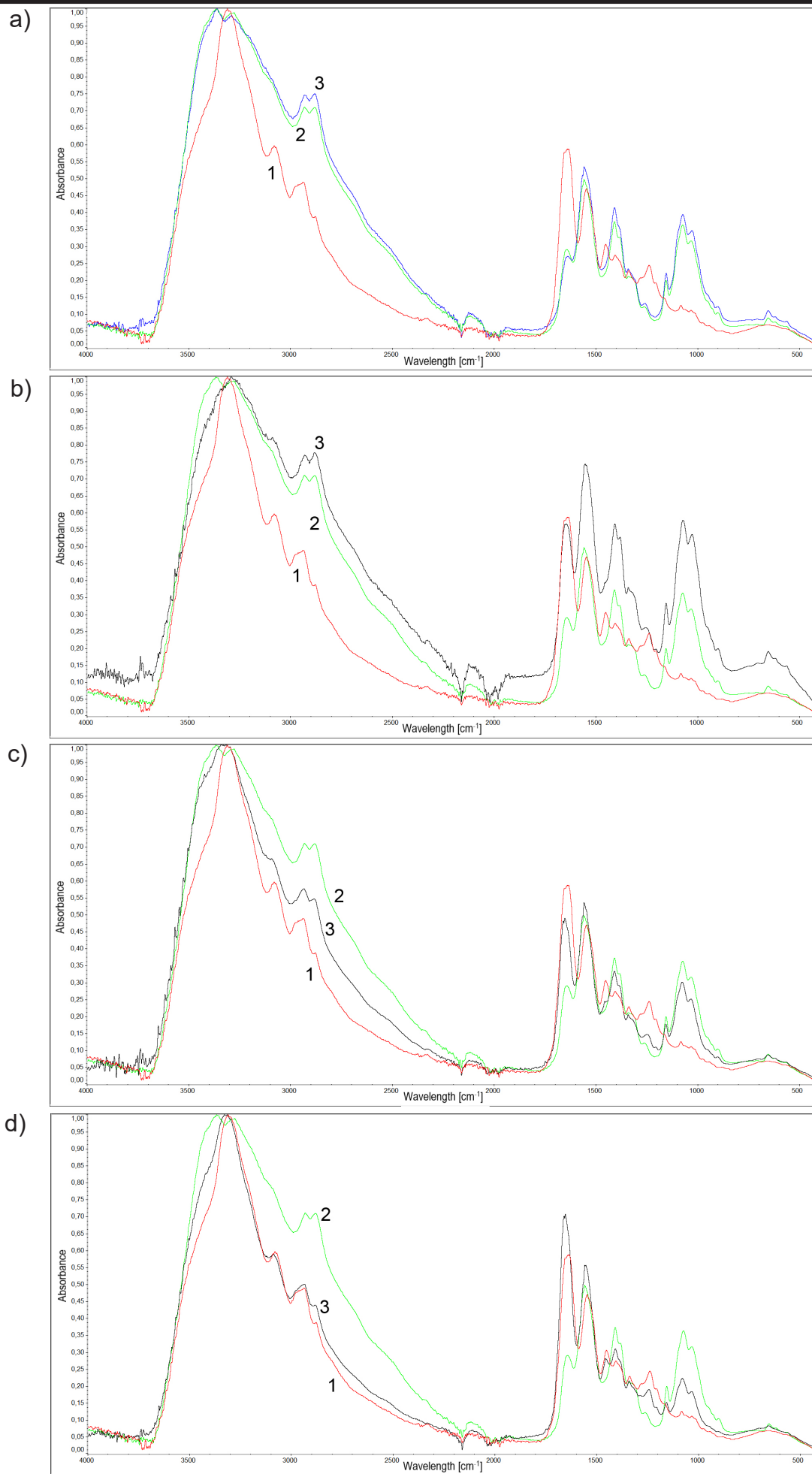
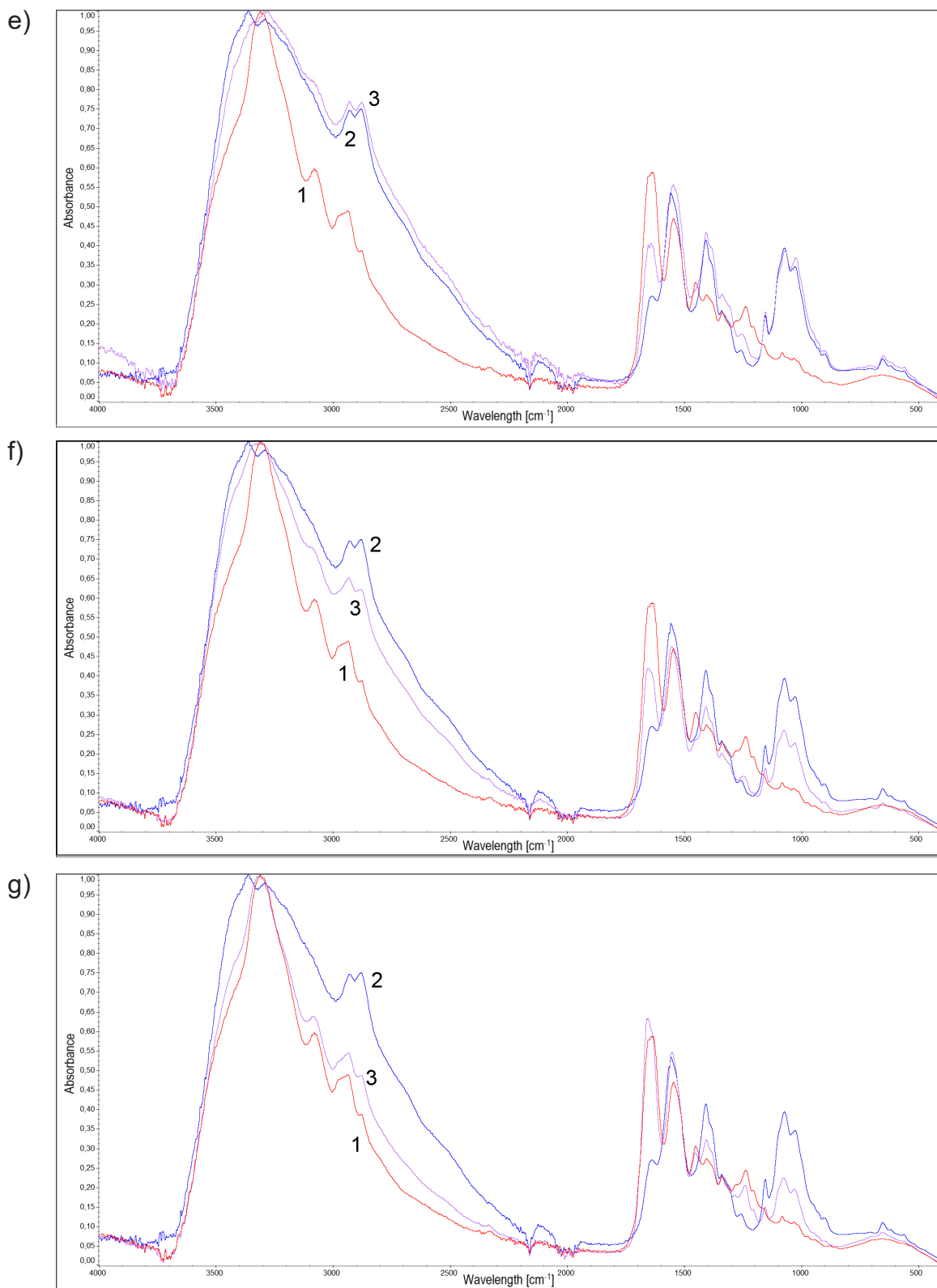ENGINEERING OF BIO MATERIALS

FIG. 1. The photographs of the polymeric thin films:
a) Col;
b) LCh;
c) 75:25 LCh-Col blend;
d) 50:50 LCh-Col blend;
e) 25:75 LCh-Col blend;
f) MCh;
g) 75:25 MCh-Col blend;
h) 50:50 MCh-Col blend;
i) 25:75 MCh-Col blend.

FIG. 2. The FTIR spectra of:
a) Col (1-red), LCh (2-green), MCh (3-blue);
b) Col (1-red), LCh (2-green), 75:25 LCh-Col blend (3-black);
c) Col (1-red), LCh (2-green), 50:50 LCh-Col blend (3-black);
d) Col (1-red), LCh (2-green), 25:75 LCh-Col blend (3-black);
e) Col (1-red), MCh (2-blue), 75:25 MCh-Col (3-violet);
f) Col (1-red), MCh (2-blue), 50:50 MCh-Col blend (3-violet);
g) Col (1-red), MCh (2-blue), 25:75 MCh-Col blend (3-violet).

TABLE 1. The characterization of mechanical properties of collagen, chitosan and chitosan-collagen blends thin films.

Material	E_{mod} [GPa]	F_{max} [MPa]	Elongation at F_{max} [mm]	F_{Bruch} [N]	Elongation at break [%]
Collagen	2.29 ± 0.87	89.17 ± 19.05	1.65 ± 0.78	23.80 ± 5.34	6.59 ± 3.16
LCh	2.90 ± 0.47	76.45 ± 10.61	0.94 ± 0.13	26.20 ± 1.63	4.78 ± 1.69
75LCh/25Col	1.78 ± 0.33	69.40 ± 16.94	2.36 ± 0.87	33.98 ± 2.27	11.03 ± 1.93
50LCh/50Col	1.33 ± 1.03	86.56 ± 21.91	0.94 ± 0.41	31.79 ± 8.33	3.77 ± 1.64
25LCh/75Col	2.58 ± 0.67	99.31 ± 7.55	2.18 ± 0.33	30.99 ± 1.36	8.71 ± 1.33
MCh	2.63 ± 0.71	98.00 ± 6.10	1.19 ± 0.16	35.54 ± 4.69	13.29 ± 8.01
75MCh/25Col	1.47 ± 0.73	75.54 ± 5.03	1.18 ± 0.08	28.62 ± 2.19	6.00 ± 1.45
50MCh/50Col	0.99 ± 0.54	75.41 ± 9.94	1.45 ± 0.31	28.94 ± 0.64	6.58 ± 1.72
25MCh/75Col	1.79 ± 0.66	84.87 ± 6.85	1.47 ± 0.53	28.99 ± 3.34	5.88 ± 2.12

TABLE 2. The glycerine and diiodomethane contact angle and surface free energy values for the collagen, chitosan and chitosan-collagen blends.

Material	Contact angle Θ (glycerine) [°]	Contact angle Θ (diiodomethane) [°]	IFT (s) [mJ/m²]	IFT (s,P) [mJ/m²]	IFT (s,D) [mJ/m²]
Collagen	60.5	56.6	37.43	15.13	22.27
LCh	72.4	58.1	31.95	8.11	23.84
75LCh/25Col	69.1	46.5	37.40	7.11	30.32
50LCh/50Col	71.6	54.5	33.57	7.63	25.94
25LCh/75Col	75.6	53.8	32.81	5.48	27.33
MCh	81.7	60.6	28.53	4.17	24.36
75MCh/25Col	75.3	59.1	30.67	6.81	23.86
50MCh/50Col	81.7	65.5	26.38	5.19	21.19
25MCh/75Col	85.3	65.1	25.83	3.59	22.24

Mechanical properties study

For each film obtained in this research, mechanical properties were measured. The results are presented in TABLE 1.

The results of the mechanical properties study indicated that the film made of pure LCh was the least deforming, ergo the stiffest. The 50:50 MCh-Col blend film was marked by the highest deformation and the lowest stiffness. The film with a 25% LCh content withstood the highest stress, while the film made of pure MCh withstood the highest breaking force. The 75% LCh film was the least resistant to the stress and the collagen film was the least resistant to the breaking force. In many cases, the values of standard deviation were high which made it difficult to decide which of the films was the most resistant to breaking. The elongation in millimetres is not proportional to the elongation percentage, ergo the conclusion about the elasticity of the studied materials is not unequivocal.

The observed variance might be caused by a slightly different sample mass and by a disparate mass of the polymers and the blends on the plates as well as by some differences in clamping the samples in the testing machine.

Contact angle measurements

Determining the contact angle informs about the quality of a material surface. The surface properties, such as roughness and wettability, are important in cosmetic and biomedical applications of biopolymer films. Wettability, i.e. the amount to which a liquid can spread on a surface, is determined by the intermolecular forces between the surface and the liquid.

TABLE 2 shows the results of the thin films surface wettability study. All of the examined biopolymer samples were marked by a glycerine contact angle below 90°, ergo it might be deduced that they are easily wettable and hydrophilic. The diiodomethane contact angle values were lower than in the case of glycerine and also lower than 90°. The reason for that might be the diiodomethane lower surface tension which lowers the contact angle. It is indicative of the more hydrophobic character of the samples, despite the earlier stated hydrophilicity. Furthermore, in the case of both liquids, the contact angles rose in the following order: collagen, LCh, and MCh. The addition of fish collagen to chitosan films caused the increase of a glycerine contact angle with the increasing content of this protein. In the case of diiodomethane, the tendency was similar, although at the lowest collagen content the contact angle value decreased.

The collagen film was marked by the lowest glycerine contact angle, ergo it was the most polar and hydrophilic. It was also confirmed by the highest value of the polar part and surface free energy. The high value of the polar part is indicative of the high polar, hydrogen, inductive, or acid-base interactions contribution between the biopolymers' molecules in the blends. In view of the mentioned properties, the collagen film might be marked by the highest adhesion to the skin which is hydrophobic. The 25:75 MCh-Col film is the least polar and hydrophilic one, which is also confirmed by the highest glycerine contact angle and the lowest value of the polar part and surface free energy. It is indicative of the mentioned film's lowest adhesion to the skin.

Diiodomethane is a liquid with a preponderant dispersive part. The film with a 75% LCh content was marked by the lowest diiodomethane contact angle, which speaks to the fact that there is the highest dispersive interactions contribution between the biopolymers in this blend. It finds its confirmation in the highest value of the dispersive surface free energy. The least dispersive interactions appear in the 50:50 MCh-Col film, which is also confirmed by the lowest value of the dispersive part.

Topography imaging

The images of the surface topography structure of the studied thin films are presented below (FIG. 3). The values of the surface roughness are listed in TABLE 3.

The surface of the studied thin films is very diverse, whereby the films made of pure biopolymers were marked by a much lower roughness than the films made of the polymer blends (TABLE 3). The AFM analysis indicated that the collagen addition to the chitosan films modifies the roughness without a specific relationship. The films made of MCh-Col blends have a less rough surface than the films made of LCh-Col blends, which might be indicative of better miscibility, and thereby of a higher homogeneity of the first ones.

TABLE 3. The R_q and R_a parameters of collagen, chitosan and chitosan-collagen blend thin films.

Material	Rq [nm]	Ra [nm]
Collagen	7.78	6.10
LCh	5.92	2.60
75LCh/25Col	63.3	45.4
50LCh/50Col	70.8	56.7
25LCh/75Col	67.3	52.9
MCh	5.19	3.99
75MCh/25Col	34.2	23.5
50MCh/50Col	28.2	22.1
25MCh/25Col	58.4	45.7
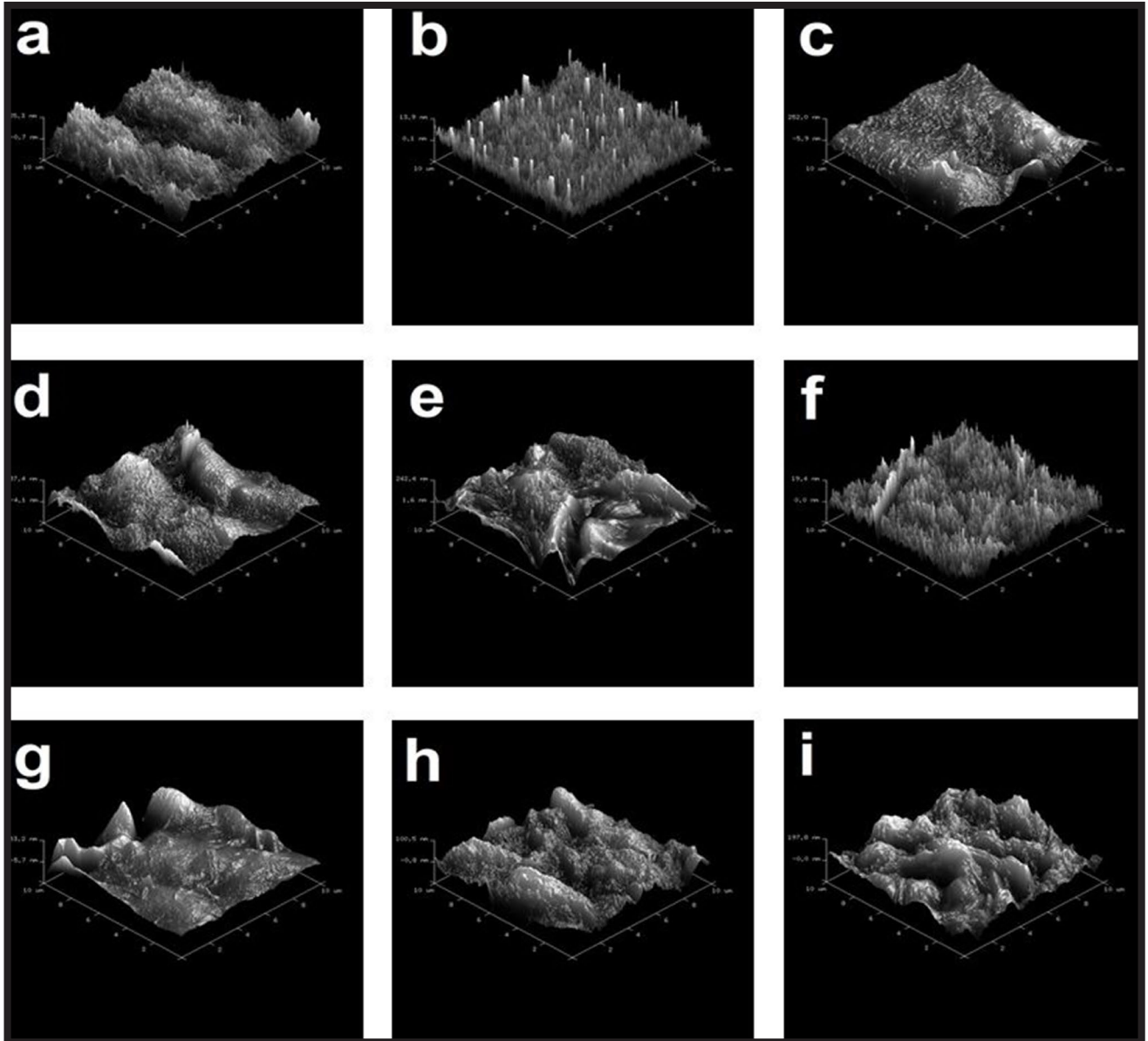
FIG. 3. The AFM images of: a) Col; b) LCh; c) 75:25 LCh-Col blend; d) 50:50 LCh-Col collend; e) 25:75 LCh-Col blend; f) MCh; g) 75:25 MCh-Col blend; h) 50:50 MCh-Col blend; i) 25:75 MCh-Col blend.
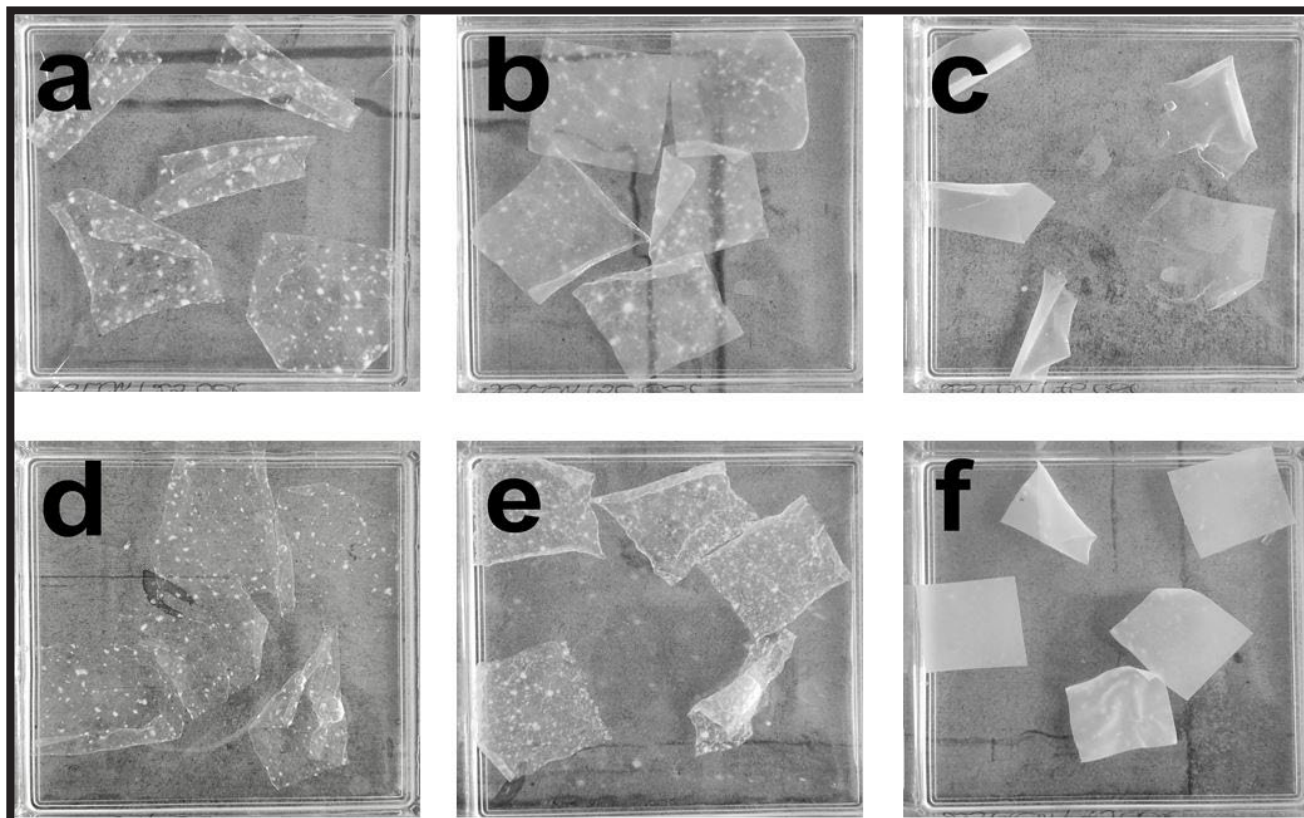
FIG. 4. The photographs of thin films samples after 1 h in PBS solution: a) 75:25 LCh-Col; b) 50:50 LCh-Col; c) 25:75 LCh-Col; d) 75:25 MCh-Col; e) 50:50 MCh-Col; f) 25:75 MCh-Col.

Swelling test

The pictures of thin films samples in PBS solution after soaking for 1 hour are presented below (FIG. 4).

The swelling tests indicated that chitosan absorbs more water than collagen, as the chitosan film samples increased their size while soaking much more than the fish collagen samples. After 1 h of soaking in PBS solution, almost all the samples fell apart while taking them out of the solution. Only a few ones made of collagen and blends with 75% collagen content remained integral for up to 4 h.

Conclusions

The interactions between collagen from skins of Silver carp and chitosan have been confirmed by IR spectra. The addition of fish collagen to chitosan films variously alters their mechanical properties. All of the studied thin films show good wettability and a hydrophilic character. The fish collagen film is marked by the highest hydrophilicity and polarity, while the 25:75 MCh-Col film is marked by the lowest hydrophilicity and polarity. The roughness of the films made of the blends is higher than the roughness of the films made of pure biopolymers and it changes irregularly, depending on the collagen content. The surface roughness of the thin films might be modified by altering the biopolymers ratio in the blend or the chitosan molecular weight.

Acknowledgments

ORCID iD

A. Sionkowska: https://orcid.org/0000-0002-1551-2725
K. Musiał: https://orcid.org/0000-0002-3596-602X
M. Gadomska: https://orcid.org/0000-0001-9214-8931
K. Adamiak: https://orcid.org/0000-0002-2386-603X

References

[1] Sionkowska A., Lewandowska K.: Biopolimery (2016). Accessed: Jan. 24, 2022. [Online]. Available: https://repozytorium.umk.pl/handle/item/3016

[2] Sionkowska A.: Current research on the blends of natural and synthetic polymers as new biomaterials: Review. Progress in Polymer Science (Oxford) 36 (2011) 1254-1276.

[3] Sionkowska A., Lewandowska K., Grabska S., Kaczmarek B., Michalska M.: Physico-chemical properties of three-component mixtures based on chitosan, hyaluronic acid and collagen. Molecular Crystals and Liquid Crystals 640 (2016) 21-29.

[4] Mohan S., Oluwafemi O.S., Kalarikkal N., Thomas S., Songca S.P.: Biopolymers – Application in Nanoscience and Nanotechnology, (2016). London: IntechOpen.

[5] Gaspar-Pintiliescu A., Stanciuc A.M., Craciunescu O.: Natural composite dressings based on collagen, gelatin and plant bioactive compounds for wound healing: A review. International Journal of Biological Macromolecules 138 (2019) 854-865.

[6] Avila Rodríguez M.I., Rodríguez Barroso L.G., Sánchez M.L.: Collagen: A review on its sources and potential cosmetic applications. Journal of Cosmetic Dermatology 17 (2018) 20-26.

[7] Sionkowska A.: Collagen blended with natural polymers: Recent advances and trends. Progress in Polymer Science 122 (2021) 101452.

[8] Zhang J., Duan R., Tian Y., Konno K.: Characterisation of acid-soluble collagen from skin of silver carp (Hypophthalmichthys molitrix). Food Chemistry 116 (2009) 318-322.

[9] Liu D., Zhou P., Li T., Regenstein J.M.: Comparison of acid-soluble collagens from the skins and scales of four carp species. Food Hydrocolloids: 41 (2014) 290-297.

[10] Faralizadeh S., Rahimabadi E.Z., Bahrami S.H., Hasannia S.: Extraction, characterization and biocompatibility evaluation of collagen from silver carp (Hypophthalmichthys molitrix) skin by-product. Sustainable Chemistry and Pharmacy 22 (2021)

[11] Sionkowska A., Adamiak K., Musial K., Gadomska M.: Collagen based materials in cosmetic applications: A review. Materials 13 (2020) 1-15.

[12] Sionkowska A., Lewandowska K., Adamiak K.: The influence of uv light on rheological properties of collagen extracted from silver carp skin. Materials 13 (2020) 1-10.

[13] Sionkowska A., Wisniewski M., Skopinska J., Kennedy C.J., Wess T.J.: Molecular interactions in collagen and chitosan blends. Biomaterials 25 (2004) 795-801.

[14] Kaczmarek B., Sionkowska A.: Chitosan/collagen blends with inorganic and organic additive - A review. Advances in Polymer Technology 37 (2017) 2367-2376.

[15] Haifei S., Xingang W., Shoucheng W., Zhengwei M., Chuangang Y., Chunmao H.: The effect of collagen-chitosan porous scaffold thickness on dermal regeneration in a one-stage grafting procedure. Journal of the Mechanical Behavior of Biomedical Materials: 29 (2014) 114-125.

[16] Li W., Long Y., Liu Y., Long K., Liu S., Wang Z., Wang Y., Ren L.: Fabrication and characterization of chitosan-collagen crosslinked membranes for corneal tissue engineering. Journal of Biomaterials Science, Polymer Edition 25 (2014) 1962-1972.

[17] Bi L., Cao Z., Hu Y., Song Y., Yu L., Yang B., Mu J., Huang Z., Han Y.: Effects of different cross-linking conditions on the properties of genipin-cross-linked chitosan/collagen scaffolds for cartilage tissue engineering. Journal of Materials Science: Materials in Medicine 22 (2011) 51-62.

[18] Sun Y., Yang C., Zhu X., Wang J. J., Liu X.Y., Yang X.P., An X.W., Liang J., Dong H.J., Jiang W., Chen C., Wang Z.G., Sun H.T., Tu Y., Zhang S., Chen F., Li X. H.: 3D printing collagen/chitosan scaffold ameliorated axon regeneration and neurological recovery after spinal cord injury. Journal of Biomedical Materials Research - Part A 107 (2019) 1898-1908.

[19] Wang D., Wang M., Wang A., Li J., Li X., Jian H., Bai S., Yin J.: Preparation of collagen/chitosan microspheres for 3D macrophage proliferation in vitro. Colloids and Surfaces A: Physicochemical and Engineering Aspects: 572 (2019) 266-273.

[20] Sionkowska A., Kaczmarek B., Michalska M., Lewandowska K., Grabska S.: Preparation and characterization of collagen/chitosan/hyaluronic acid thin films for application in hair care cosmetics. Pure and Applied Chemistry 89 (2017) 1829-1839.

[21] Brower V.: The biochemistry of beauty. The science and pseudo-science of beautiful skin. EMBO Reports 3 (2002) 712-714.

[22] Guillerme J.B., Couteau C., Coiffard L.: Applications for marine resources in cosmetics. Cosmetics 4 (2017) 1-15.

[23] Thongchai K., Chuysinuan P., Thanyacharoen T., Techasakul S., Ummartyotin S.: Characterization, release, and antioxidant activity of caffeic acid-loaded collagen and chitosan hydrogel composites. Journal of Materials Research and Technology 9 (2020) 6512-6520.

[24] Sharkawy A., Barreiro M.F., Rodrigues A.E.: New Pickering emulsions stabilized with chitosan/collagen peptides nanoparticles: Synthesis, characterization and tracking of the nanoparticles after skin application. Colloids and Surfaces A: Physicochemical and Engineering Aspects 616 (2021)

[25] Schlotmann K., Kaeten M., Black A.F., Damour O., Waldmann-Laue M., Förster T.: Cosmetic efficacy claims in vitro using a three-dimensional human skin model. International Journal of Cosmetic Science 23 (2001) 309-318.

PROPERTIES OF COATINGS USED IN BIOTRIBOLOGICAL SYSTEMS

Katarzyna Piotrowska[1]* [iD], Monika Madej[1] [iD],
Magdalena Niemczewska-Wójcik[2] [iD]

[1] Kielce University of Technology,
Mechanical Department,
al. Tysiąclecia P. P. 7, 25-314 Kielce, Poland
[2] Cracow University of Technology,
Mechanical Department,
al. Jana Pawła II 37, 31-864 Kraków, Poland
*e-mail: kpiotrowskapsk@gmail.com

Abstract

The properties of diamond-like carbon coatings (DLC) obtained via plasma-assisted chemical vapor deposition (PACVD) on the Ti13Nb13Zr alloy were evaluated. For this purpose, measurements of the thickness, the surface geometric structure, adhesion, as well as tribological tests of the tested coatings were performed. The thickness of the deposited coating was measured using the spherical grinding method. Surface geometry measurements before and after tribological tests were performed with a Leica DCM8 optical profilometer. A scratch test was performed to measure the adhesion of the coating. An indenter with a Rockwell geometry was used during the adhesion tests. The test offered the possibility of real-time recording of the coefficient of friction and acoustic emission. In addition, it was also possible to measure the geometrical parameters of a scratch and to carry out a microscopic analysis of a scratch during the coating damage. The test was carried out on an Anton Paar MCT³ instrument. The model tribological tests were carried out in rotary motion under technically dry friction conditions and friction conditions with lubrication with the Ringer's solution and an artificial saliva solution. The tests were carried out using an Anton Paar TRB³ tribometer. The scratch test proved that the deposited layer was characterized by good adhesion. Based on the results of the tribological tests, it was found that the lower resistance to motion and wear was obtained for the DLC coatings on the Ti13Nb13Zr substrate. The results of the tests performed on the DLC coatings indicate the possibility of their application in biotribological systems.

***Keywords:** PACVD technique, titanium alloys, surface texture, hardness, friction, wear*

Introduction

The increase in demand for modern biomaterials has led to the rapid development of implantology. Implants, in addition to appropriate mechanical properties, must be highly biocompatible and resistant to bacteria and fungi. This poses a huge challenge to modern materials science. In this context, one of the most often studied classes of materials are carbon materials, including diamond-like carbon (DLC) coatings [1-3]. Compared to commonly used anti-wear layers, DLC coatings are characterized by high resistance to wear by friction, high adhesion to the substrate, high hardness, and high thermal and chemical stability [4-7]. DLC coatings are mixtures of amorphous carbon with sp^3 and sp^2 bonds. Hybridisation of sp^3, which is characteristic of the diamond, results in increased resistance to abrasion and hardness, and good thermal conductivity. The sp^2 bonds derived from graphite determine the low resistance to motion values. The carbon hybridisation degree, the mixture composition, and the physicochemical properties of a DLC coating are determined by the selected production method and the production process conditions [8-11]. Carbon coatings are obtained via classical chemical methods which are multi-step and labour-intensive. The surface modification of biomaterials via plasma provides completely new possibilities for tailoring their surface properties to specific applications. In this paper, the authors examined the properties of diamond-like carbon coatings obtained via plasma-assisted chemical vapour deposition (PACVD) in terms of their use in biotribological systems.

Materials and Methods

The subject of the study was the Ti13Nb13Zr titanium alloy with the chemical composition shown in TABLE 1 and the mechanical properties summarised in TABLE 2.

Disks made of the Ti13Nb13Zr titanium alloy with a diameter of 30 mm and a height of 6 mm were processed using a grinding-polishing machine made by Pace Technologies. Silicon carbide abrasive papers with increasing grain size from 120 to 2500 µm were used. The finishing treatment involved polishing on cloth with the addition of a polishing slurry with Al_2O_3, with a grain size of 0.05 µm. After grinding and polishing, the sample surface roughness value of Ra = 0.06 µm was obtained. The other amplitude parameters of the reference surface are shown in TABLE 6. Before coatings were deposited, the samples were degreased in ethanol in an ultrasonic cleaner. A DLC coating was deposited on the prepared material by plasma-assisted chemical vapour deposition (PACVD).

The thickness of the coating was determined using a Calotest device. A steel ball of 20 mm in diameter, rotated on the surface of the coating at the speed of 3000 rpm. The duration of the test was 1240 s. During the test, a diamond paste with a small grain size of < 0.2 µm was used. A diagram of the friction pair in the Calotest device is shown in FIG. 1a. As a result of friction, the material from both the coating and the substrate was removed. The geometric traces of the removed coating and the substrate material had the shape of concentric circles. To determine the thickness of the coating, the diameters of the circles were measured using an optical microscope (FIG. 2). The test was repeated 5 times.

The geometric structure was examined using confocal microscopy. The measurement involved scanning the surface of the tested materials over an area measuring 1.2 mm x 1.6 mm.

Tribological tests were carried out on a TRB[3] tribometer of the ball-on-disc type in rotary motion in technically dry friction conditions and in conditions of friction with lubrication with the Ringer's fluid and with an artificial saliva solution, with constant parameters of the friction pair (TABLE 3). The chemical composition of the lubricants is shown in TABLE 4. The counter samples in the examined friction pairs were Al_2O_3 balls with a diameter of 6 mm. A photograph of a friction pair is shown in FIG. 1b.

The primary method used to determine the coating quality is the evaluation of a mechanical indicator, namely adhesion. The advantage of adhesion testing is that the changes in the coefficient, the friction force, and the acoustic emission can be recorded in real-time. In addition, it is also possible to measure the geometric parameters of a scratch and to perform microscopic analysis of a scratch during coating damage. The technical parameters of the scratch test are shown in TABLE 5.

TABLE 1. Chemical composition of Ti13Nb13Zr titanium alloy, % weight.

Element	% weight							
	C	H	O	N	Fe	Nb	Zr	Ti
Ti13Nb13Zr	≤ 0.08	≤ 0.015	≤ 0.016	≤ 0.05	≤ 0.25	12.5-14.0	12.5-14.0	based

TABLE 2. Mechanical properties of the Ti13Nb13Zr alloy.

Material	Rm [MPa]	Re [MPa]	A [%]	Z [%]	E [GPa]
Ti13Nb13Zr	973-1037	836-908	10-16	27-53	79-84
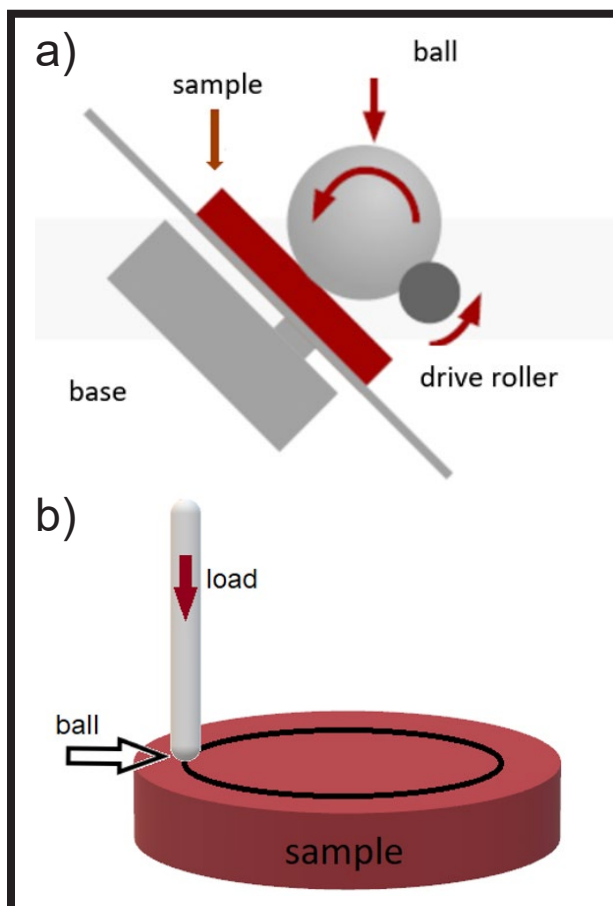
FIG. 1. Friction pair in Calotest (a), friction pair in TRB[3] (b).

TABLE 3. Technical and environmental parameters of the tribological test.

Parameter	Unit	Friction pair ball Al_2O_3 – disk Ti13Nb13Zr ball Al_2O_3 – disk Ti13Nb13Zr DLC
Load	N	5
Linear speed	m/s	0.1
Friction path	m	1 000
Radius	mm	11
Cycle	-	14 458
Humidity	%	50 ± 1
Temperature	°C	23 ± 1
Lubricant	-	- Ringer solution Artifical saliva

TABLE 5. Technical parameters of mechanical test.

	Adhesion
Device	MHT[3]
Indenter	Diamond Rockwell
Load	0.03-30 N
Loading rate	10046.65 mN/min
Unloading rate	-
Scratch length	2 mm

TABLE 4. Chemical composition of the lubricants.

	Chemical composition [g/dm³]						
	NaCl	KCl	$CaCl_2$	$CaCl_2 \cdot 2H_2O$	$NaH_2PO_4 \cdot 2H_2O$	$Na_2S \cdot 9H_2O$	Urea
Ringer solutions	8.6	0.3	0.243	-	-	-	-
Artificial saliva	0.4	0.4	-	0.906	0.690	0.005	1.0

Results and Discussion

The thickness of the diamond-like carbon coating was measured using optical microscopy. The resulting layer was 1.77 µm thick. FIG. 2 shows an abrasion mark.

FIG. 3 shows the results of the examination of the surface geometric structure. The study presents the axonometric images and the surface profiles of both the reference sample and the DLC coating. The average profiles for each sample were generated based on 100 profiles. The amplitude parameters (acc. to ISO 4287) are shown in TABLE 6.

Examinations of the surface geometric structure revealed that the deposition of a diamond-like carbon coating on the Ti13Nb13Zr alloy did not change the values of the amplitude parameters (there was a slight increase in the Rp Rv, Ra, and Rq indices). Additional information on the surface shape of the studied samples was obtained by determining the coefficient of surface inclination (asymmetry) Rku and the clustering coefficient Rsk. Both parameters are very sensitive to the presence of local elevations, depressions, and defects on the surface. A negative value of Rsk indicates that the surface of the reference sample is flat. If the index for the coating reaches 0.49, the emergence of steep elevations with sharp tops is demonstrated.

FIG. 4 shows the results of the adhesion tests. The critical force was evaluated based on the microscopic observations and the recorded changes in the friction coefficient and the acoustic emission.

Based on the plot of the friction coefficient (µ) and the acoustic emission, it was found that the first cracks in the coating appeared under a load equal to 3.6 N (LC1). Microscopic analysis of the crack at this location showed no changes in the coating structure. When the force of 8.1 N (LC2) was exceeded, a sharp increase in the acoustic emission values was observed. The microscopic image showed the first chipping at the edge of the scratch. The scratch test of the diamond-like carbon coating revealed that the deposited layer became delaminated under the load of 13.3 N (LC3); at the same time, the friction coefficient increased almost threefold from 0.16 (at LC2) to 0.45.
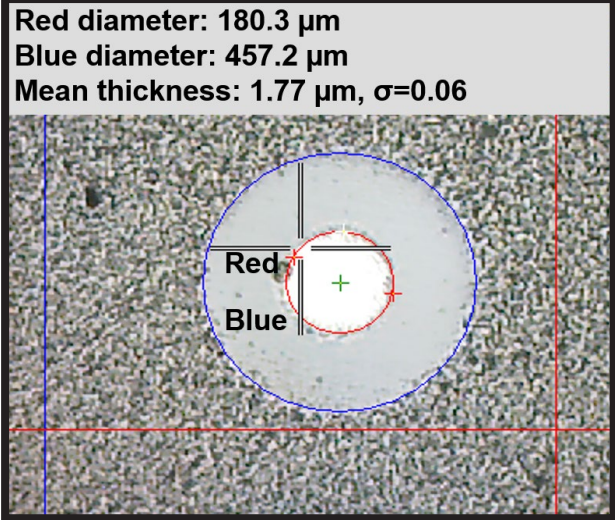
Red diameter: 180.3 µm
Blue diameter: 457.2 µm
Mean thickness: 1.77 µm, σ=0.06

Red
Blue

FIG. 2. An image recorded during thickness measurement of the DLC coating.

TABLE 6. The parameters of surface texture.

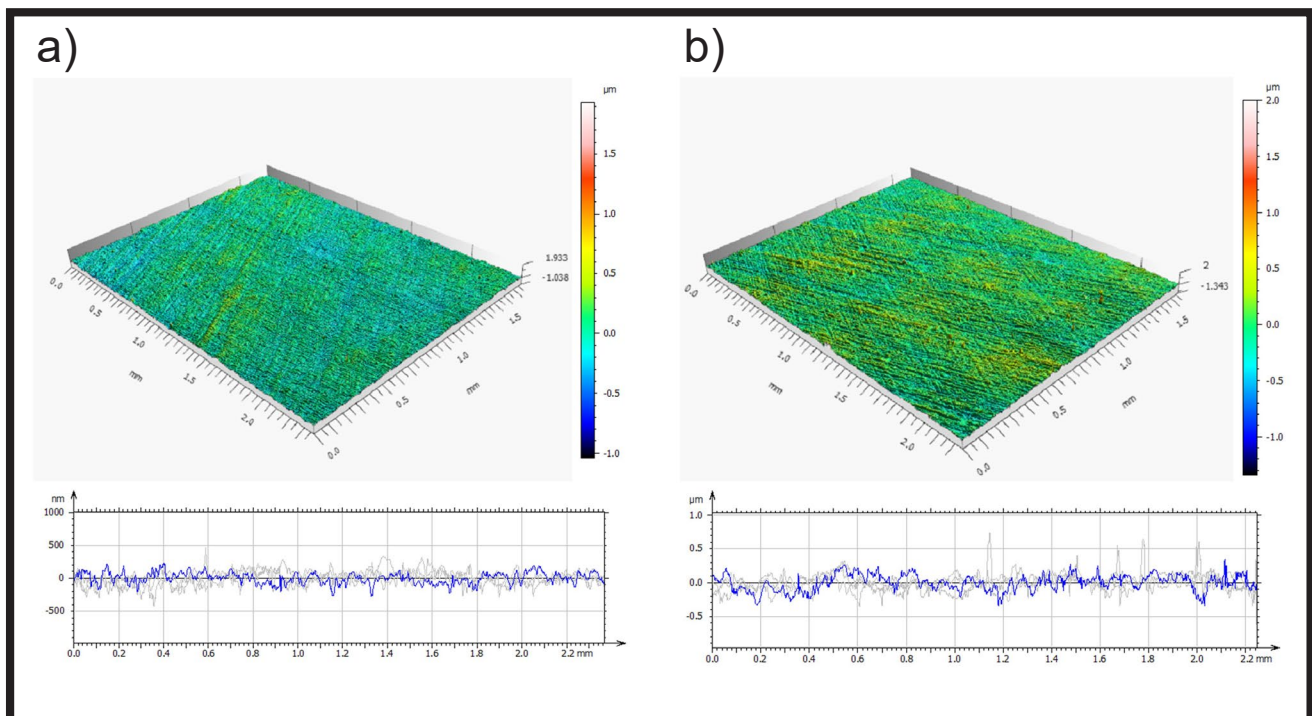| Parameter	Ti13Nb13Zr reference	Ti13Nb13Zr DLC
	mean	mean
Rp [nm]	268	348
Rv [nm]	243	244
Ra [nm]	65	73
Rq [nm]	80	90
Rsk	-0.03	0.49
Rku	3.41	4.41

a)

b)

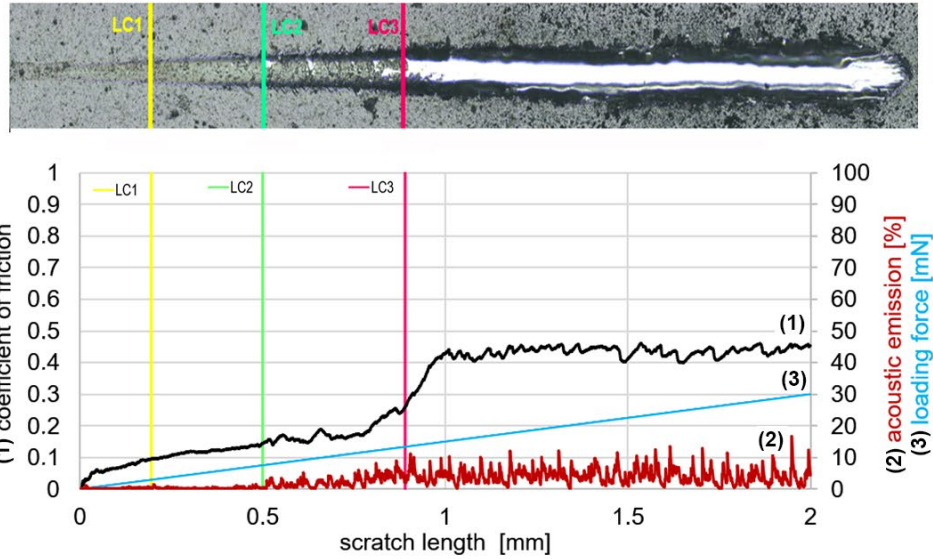**FIG. 3. The isometric image of surface and the sample profile of the surface: a) Ti13Nb13Zr, b) Ti13Nb13Zr DLC.**

FIG. 4. Scratch test results - graph of variation of loading force (Fn), coefficient of friction (μ), acoustic emission.
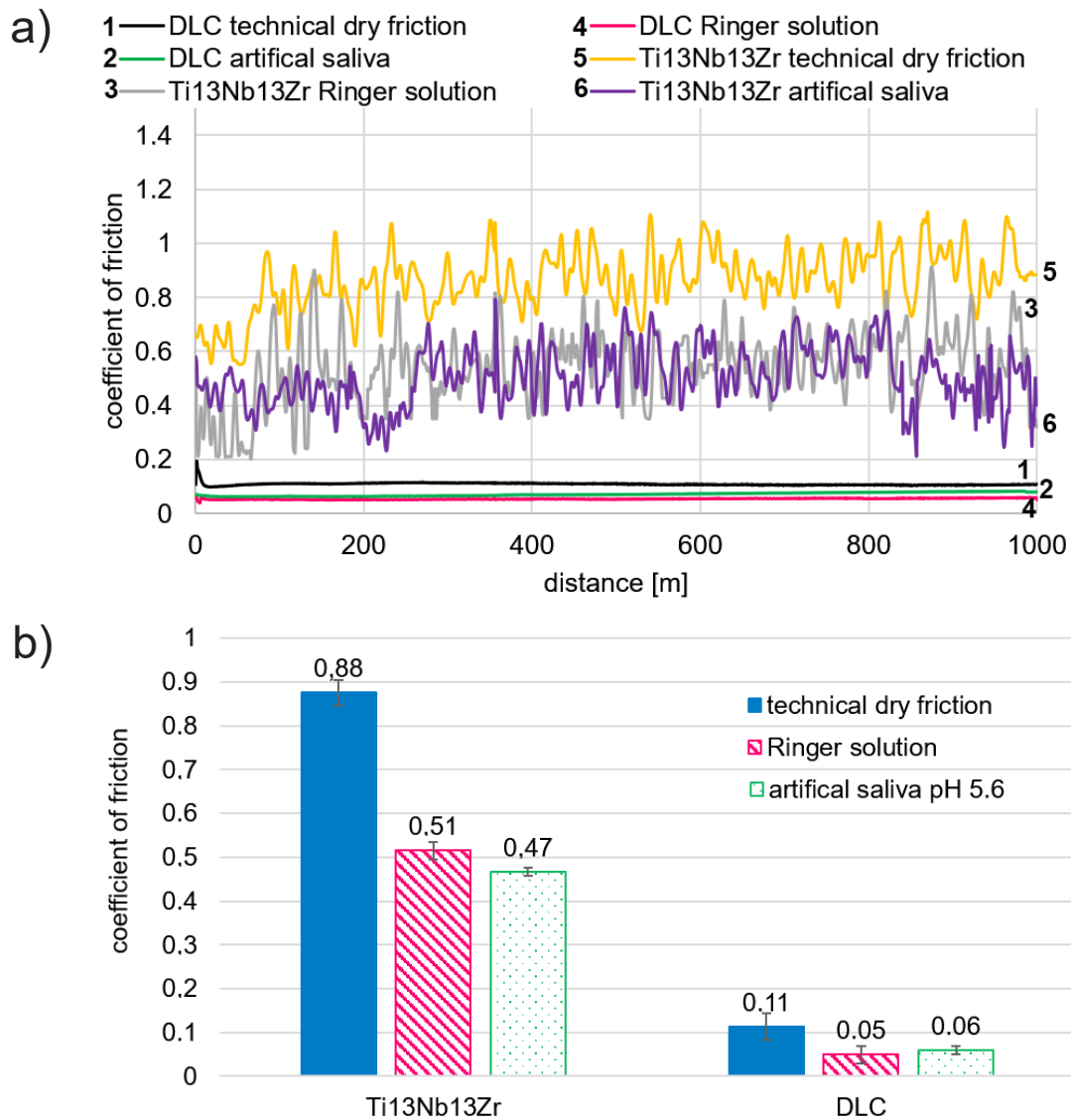

FIG. 5. a) Sample plots of the coefficient of friction, b) mean coefficient of friction.

FIG. 5a shows the sample plots of friction coefficient μ as a function of the number of recorded friction pair cycles. The values in FIG. 5b are averaged values of the friction coefficient measured during three measurement series. The diagram shows the average values of the friction coefficient calculated from three measurement series. The results of the tribological tests showed that the diamond-like carbon coating is characterized by low resistance to motion. In the case of technically dry friction, the average friction coefficient was 0.11 which was eight times lower than the Ti13Nb13Zr alloy.

Moreover, it was observed that for both the reference sample and the coated sample, the application of lubricants resulted in a reduction in the resistance to motion.

After the tribological tests, microscopic observations were performed on the samples. FIG. 6-8 shows examples of the axonometric images of abrasion marks and the abrasion profiles on a cross-section. TABLE 7 shows the average wear area for the samples on the cross-sectional area determined after five measurement series.
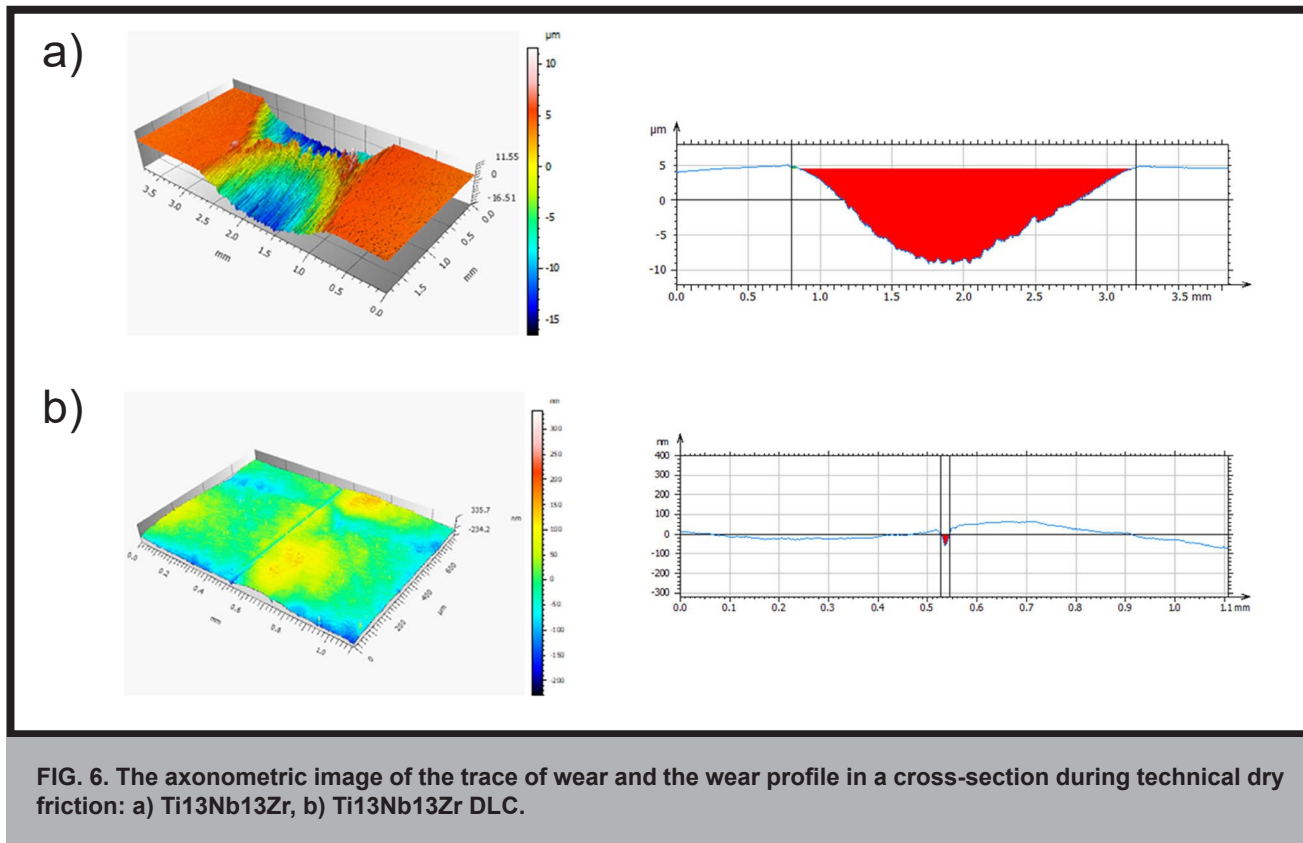

FIG. 6. The axonometric image of the trace of wear and the wear profile in a cross-section during technical dry friction: a) Ti13Nb13Zr, b) Ti13Nb13Zr DLC.
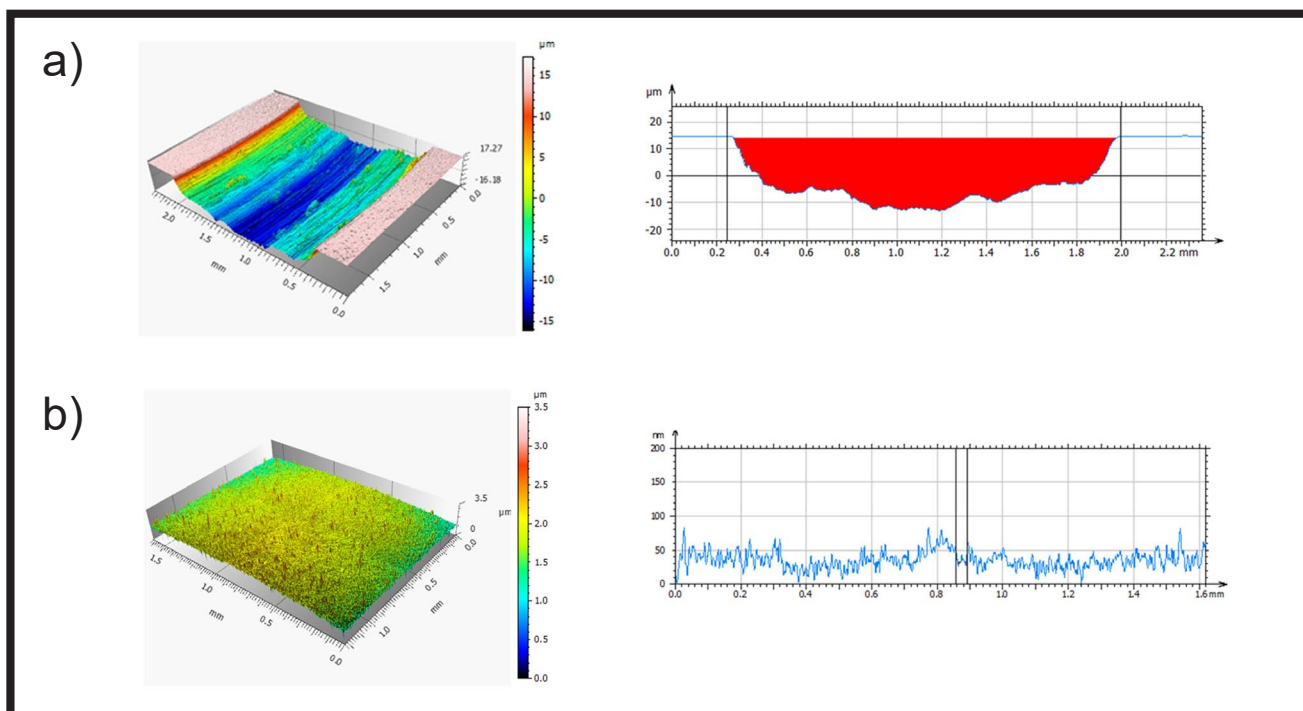

FIG. 7. The axonometric image of the trace of wear and the wear profile in a cross-section during friction in the Ringer's solution environment: a) Ti13Nb13Zr, b) Ti13Nb13Zr DLC.
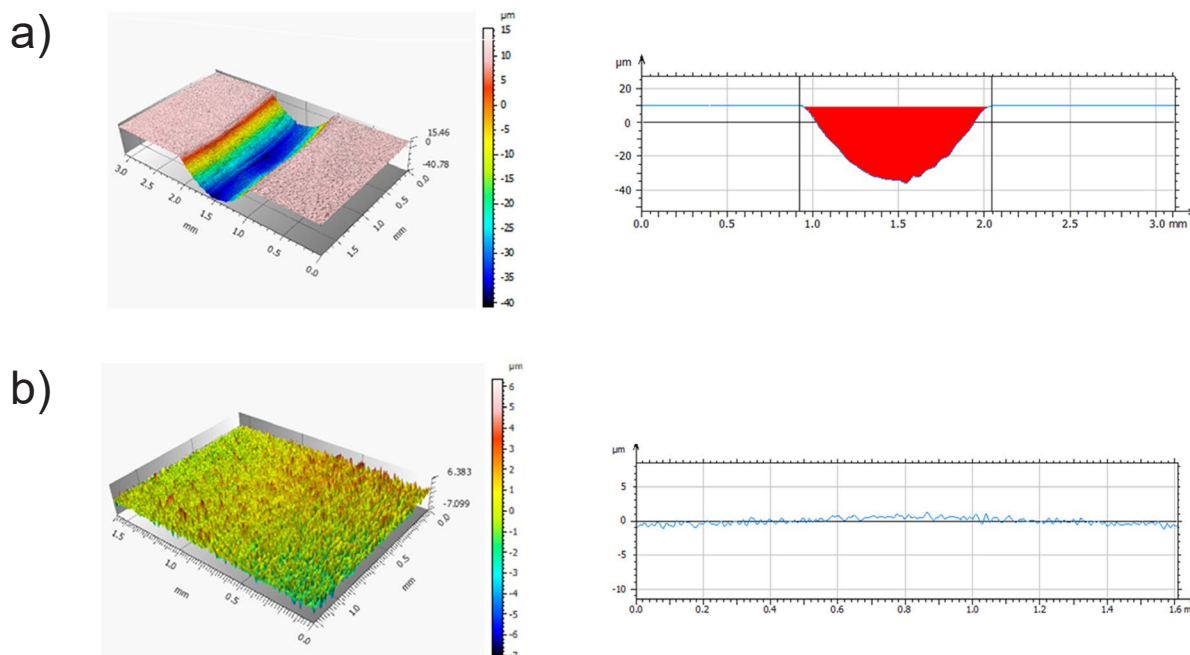
ENGINEERING OF BIOMATERIALS

FIG. 8. The axonometric image of the trace of wear and the wear profile in a cross-section during friction in an artificial saliva environment: a) Ti13Nb13Zr, b) Ti13Nb13Zr DLC.

TABLE 7. Average wear area on the cross-section.

	Ti13Nb13Zr	Ti13Nb13Zr DLC
Technical dry friction	17 000 000 µm^2	0.54 µm^2
Ringer solution	34 000 000 µm^2	0.08 µm^2
Artificial saliva	31 000 000 µm^2	0.05 µm^2

The analysis of the surface geometric structure examinations after the tribological tests showed that the Ti13Nb13Zr titanium alloy had lower wear resistance compared to the DLC coating. It was observed that the use of lubricants in the case of the Ti13Nb13Zr resulted in an almost twofold increase in wear. Most likely, the reason for the increased wear of the titanium alloy was the presence of chloride ions (Cl$^-$) contained in the lubricants, both the Ringer's solution and the artificial saliva. In the case of the DLC coating, there was a reduction in wear after the application of the lubricants, which was probably associated with the passive nature of the coating. The analysis of axonometric images of the reference sample indicated the presence of numerous free wear products on the tested surfaces, which intensified the wear processes.

Conclusions

The tested DLC coating deposited on the Ti13Nb13Zr titanium alloy, using the PACVD technique, was 1.77 µm thick. The examination of the surface geometric structure showed that the amplitude indices did not change significantly as a result of the coating deposition. The scratch test revealed that the deposited layer was characterized by the high adhesion. The tribological tests proved that the DLC coating was characterized by the low resistance to motion and that the use of lubricants reduced this index almost twofold. The highest friction coefficient was obtained during the technically dry friction of the Ti13Nb13Zr - Al$_2$O$_3$ friction pair. It was eight times higher than the values recorded for the coating. The results of the friction-wear tests indicated that the Ti13Nb13Zr titanium alloy was characterized by the lower resistance to wear by friction than the DLC coating, and the lubricants application increased its wear almost twofold.

Acknowledgements

ORCID iD

K. Piotrowska: https://orcid.org/0000-0001-6366-2755
M. Madej: https://orcid.org/0000-0001-9892-9181
M. Niemczewska-
Wójcik: https://orcid.org/0000-0001-9902-478X

References

[1] Piotrowska K., Madej M., Granek A.: Assessment of Mechanical and Tribological Properties of Diamond-Like Carbon Coatings on the Ti13Nb13Zr Alloy. Open Engineering 10 (2020) 536-545.

[2] Batory D., Gorzędowski J., Kołodziejczyk Ł., Szymański W.: Modification of diamond-like carbon coatings by silver ion implantation. Engineering of Biomaterials 14 105 (2011) 5-12.

[3] Świątek L., Olejnik A., Grabarczyk J.: The influence of the DLC and DLC-Si coatings on the changes occurring on the implants surface during the implant-bone contact. Engineering of Biomaterials 19 137 (2016) 2-12.

[4] Robertson J.: Diamond-like amorphous carbon. Materials Science and Engineering: R: Reports 37 4–6 (2002) 129-282.

[5] Donnet C., Fontaine J., Mogne T., et al.: Diamond-like carbon-based functionally gradient coatings for space tribology. Surface & Coatings Technology 120-121 (1999) 548-554.

[6] Yun D.Y., Choi W.S., Park Y.S., Hong B.: Effect of H_2 and O_2 plasma etching treatment on the surface of diamond-like carbon thin film. Applied Surface Science 254 23 (2008) 7925-7928.

[7] Shirakura A., Nakaya M., Koga Y., Kodama H., Hasebe T., Suzuki T.: Diamond-like carbon films for PET bottles and medical applications. Thin Solid Films 494 1-2 (2006) 84-91.

[8] Marciniak J.: Biomateriały, wyd. Politechniki Śląskiej, Gliwice 2002.

[9] Gilewicz A., Warcholiński B.: Twarde powłoki ta-C otrzymane metodą impulsowego katodowego odparowania łukowego. Inżynieria Materiałowa 1 (2010) 50–53.

[10] Kobashi K.: Diamond films, chemical vapour deposition for oriented and heteroepitaxial growth. Elsevier 2005.

[11] Robertson J.: Diamond like amorphous carbon. Materials Science and Engineering 37 (2002) 129–281.